Universidade do Minho
Escola de Ciências

Jaime Pedro Oliveira da Silva

Study and optimization of the macroscopic electrical response of carbon based nanocomposites for advanced applications

agosto de 2013

Jaime Pedro Oliveira da Silva **Study and optimization of the macroscopic electrical response of carbon based nanocomposites for advanced applications** UMinho | 2013

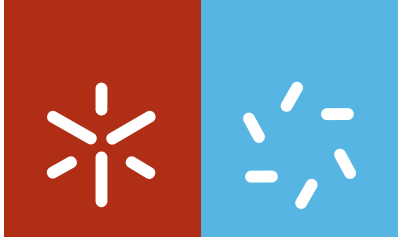

Universidade do Minho
Escola de Ciências

Jaime Pedro Oliveira da Silva

Study and optimization of the macroscopic electrical response of carbon based nanocomposites for advanced applications

Programa Doutoral em Física (MAP-fis)

Trabalho realizado sob a orientação do
Professor Doutor Senentxu Lanceros-Mendez
e co-orientação do
Professor Doutor Ricardo Simões

agosto de 2013

Nome

Jaime Pedro Oliveira da Silva

Endereço electrónico: silva.jaime@gmail.com **Telefone**: 917646313

Número do Bilhete de Identidade: 11145628

Título:

Study and Optimitization of the Macroscopic Electrical Response of Carbon Based Nanocomposites for Advanced Applications

Orientador(es):

Senentxu Lanceros Mendez, Ricardo Simões

Ano de conclusão: 2013

Designação do Doutoramento:

Programa Doutoral Map-fis

Universidade do Minho, ___/___/_____

Assinatura: _____

Acknowledgements

I would like to express my profound gratitude to Prof. Senentxu Lanceros-Mendez, for supporting, guiding, patience and friendship. I am also very grateful to Prof. Ricardo Simões, he left me free to work as I preferred, and was always available to help me, guide me and support me.

I acknowledge my gratitude to the Center of Computational Physics in the University of Coimbra for welcoming me during the writing of this thesis.

I acknowledge my gratitude also to FCT grant SFRH/BD/60623/2009 and to Prof Alberto Proença for providing the SEARCH cluster that was used in part of this work and PEst-C/CTM/LA0025/2011. Part of this work was framed in the project PTDC/CTM/69316/2006 and PTDC/EME-PME/108859/2008.

Também agradeço à minha família, Jaime, Aldina e Sofia, pelo seu constante apoio, ajuda, encorajamento, amor e carinho. Agradeço também ao Francisco pelas tardes de futebol bem passadas que ajudaram a espairecer nas fases de maior stress. Finally my deepest gratitude to my wife, Inês, for her understanding and love. Her support and encouragement has made this work possible.

Resumo

A presente tese centrou-se no estudo da resposta da constante dielétrica e condutividade elétrica em materiais compósitos nos quais o reforço tinha uma elevada proporção entre comprimento e diâmetro. O objeto de estudo foi o efeito de um reforço com uma elevada razão entre comprimento e diâmetro, concentração e orientação na resposta elétrica e dielétrica de um compósito. Estes compósitos têm uma grande importância no desenvolvimento de materiais para sensores e atuadores.

Num primeiro momento da dissertação, explorou-se a resposta da constante dielétrica de um compósito constituído por nanotubos de carbono como reforço e uma matriz polimérica. Verificou-se que um aumento da razão entre comprimento e diâmetro do reforço tem o efeito de aumentar a constante dielétrica do compósito para uma igual fração volumétrica de reforço. Constatou-se também que materiais na fase nemática demonstram uma constante dielétrica mais baixa quando comparados com materiais onde o reforço está distribuído aleatoriamente. Ficou ainda demonstrado nesta dissertação que materiais na fase nemática com razões entre o comprimento e diâmetro diferentes a constante dielétrica segue uma lei de potência.

Numa segunda fase do trabalho, foi explorada a condutividade de nanocompósitos poliméricos reforçados com nanotubos de carbono, através de um modelo baseado em cilindros impenetráveis. Ficou demonstrado que o modelo é apropriado para descrever a condutividade elétrica de um nanocompósito polimérico reforçado com nanotubos. As simulações desenvolvidas demonstram que, aumentando a razão entre o comprimento e o diâmetro dos nanotubos de carbono, aumenta a condutividade elétrica do nanocompósito. No entanto, verifica-se que aumentando a anisotropía diminui a condutividade, sendo este efeito mais evidente para frações volumétricas maiores.

Nesta dissertação comprovou-se ainda que uma microestrutura gerada por um algoritmo de empacotamento sequencial pode ser descrita por um grafo aleatório e que a condutividade num compósito reforçado com nanofibras de carbono pode ser descrito por uma rede de Bethe. Através do uso da teoria das redes complexas, chegou-se a uma expressão para o limite de percolação e, do mesmo modo, demonstrou-se que ¨hopping¨ entre fibras adjacentes resulta numa expressão que corresponde a um regime de desordem fraca.

No trabalho desenvolvido também foi calculado os expoentes críticos, através da teoria das redes, para um sistema 3D composto por cilíndros impenetráveis com uma interação de curto alcance, demonstrando que os expoentes críticos estão relacionados por um relação de hiperescala comum para 3D e não pertencem à mesma classe de universalidade como a percolação numa rede.

A aplicação do modelo desenvolvido a compósitos de epoxy reforçada, com diferentes métodos de dispersão de nanofibras de carbono, revelou que os métodos de dispersão usados para preparar os compósitos têm uma forte influência nas propriedades elétricas que podem ser capturadas pelo modelo. Neste contexto, ficou ainda demonstrado que a condutividade elétrica pode ser descrita por um regime de desordem fraca, isto é, um regime onde todas as conexões fibra-fibra participam na condutividade do compósito.

O modelo desenvolvido foi aplicado igualmente a compósitos de poly (vinylidene fluoride) reforçado com nanotubos de carbono com diferentes tratamentos de térmicos de oxidação. Verificou-se que os tratamentos de superfície aumentam o limite de percolação e diminuem a condutividade. Nesta dissertação provámos ainda que a condutividade do compósito pode ser atribuída a um mecanismo de ¨hopping¨, fortemente afetado pelos tratamentos de superfície dos reforços.

Abstract

This thesis studies the dielectric constant and electrical conductivity of polymer composites with embedded high aspect ratio fillers. It is mainly focussed on the influence of the aspect ratio, filler concentration and orientation on the electrical response of the composite. These composites are of large importance in the development of materials for sensor and actuators.

The thesis starts by exploring the dielectric constant of carbon nanotube/polymer composites. It was found that an increase of the aspect ratio of the fillers increases the dielectric constant of the nanocomposite for a given volume fraction. It was also demonstrated that nematic materials show a lower dielectric constant when compared to isotropic ones. It was concluded that for nematic state materials with different aspect ratios, the dielectric constant follows a power law.

The conductivity of carbon nanotube/polymer nancomposites was also addressed by using a model based on "hard-core" cylinders and it was demonstrated that simulations based on hard-core cylinders can describe the conductivity of the nanocomposites. It was demonstrated that increasing aspect ratio increases the electrical conductivity and that increasing the anisotropy will decrease conductivity; this effect being more evident at higher volume fractions.

It was also shown that the microstructure generated by a derivation of sequential packing algorithm can be described by a random graph and that the electrical conduction in carbon nanofiber/polymer composites can be described by a Bethe lattice. Through the use of the complex network framework, an expression is obtained for the percolation threshold. In the same way, it was demonstrated that "hopping" between adjacent fillers results on an expression that corresponds to a weak disorder regime.

The critical exponents for a hard-core 3D cylinder system with short-range interaction were calculated, making use of the network theory. It was demonstrated that these are related through the common hyperscaling for a 3D system and do not belong to the same universality class as the lattice percolation.

The application of the developed model to carbon nanofiber/Epoxy composites prepared with different carbon nanofiber dispersion methods, reveals that the dispersion methods induce a strong influence on the composite electrical properties that can be captured by the model. It is also found that the electrical conductivity can be described by a weak disorder regime, a regime where all fiber-fiber conductive links participate in the overall composite conductance.

The model was also applied to carbon nanotube/poly(vinylidene fluoride) composites prepared using fillers with different oxidation and ther-

mal treatments. The surface treatments, in general, increase the percolation threshold and decrease conductivity. It was also demonstrated that the composite conductivity can be attributed to a hopping mechanism that is strongly affected by the surface treatment of the fillers.

List of Figures

Contents

List of abbreviations, acronyms and symbols

AR	Aspect Ratio
CB	Carbon Black
CF	Carbon Fiber
CNT	Carbon Nanotube
D	Cylinder diameter
Eq.(s)	Equation (s)
Fig.	Figure
FSS	Finite size scaling analysis
G_{cut}	System effective conductance before being conductive
G_{eff}	Composite effective conductance
h	Planck's constant
k_B	Boltzmann's constant
L	Cylinder length
ℓ_{opt}	Optimal path
MPI	Message Passing Interface
MWCNT	Multi Wall Carbon Nanotube
nm	Nanometer
ϕ_c	Percolation threshold
PVDF	Poly(vinylidene fluoride)
RC	Resistor capacitor network
V_e	Excluded volume
VGCNF	Vapour Grown Carbon Nanofiber
$< z >$	Average degree of a graph
δ_{max}	Maximum value for the minimum separation distance
μm	Micrometre
σ	Electrical Conductivity
σ_{AC}	Alternate current conductivity
σ_{DC}	Direct current conductivity
ϕ	Filler volume fraction
ξ	Correlation length

1

Introduction

The addition of carbon allotropes to a polymeric matrix, producing a composite, is known to affect its mechanical and electrical properties. The changes can be significant even at small weight fractions of the reinforcement [1, 2]. One of the most important steps in designing a polymer composite for specific applications is to understand the way in which its physical properties depend on the composite characteristics. For applications where the focus is the composite electrical conductivity or the composite dielectric constant it is fundamental to choose the type of fillers. Carbonaceous fillers like carbon black (CB), carbon nanotubes (CNT) or vapour grown carbon nanofibers (VGCNF) are well known to increase the electrical properties of a polymeric matrix[2]. Among the carbon's allotropes, CNT and VGCNF are characterized by a length that is in the order of μm for VGNF[3, 2] and from nm to μm for CNT[3, 2]. The CNT and VGCNF diameter has a dimension at the nm scale, hence, the latter fillers have an high aspect ratio, $AR = length/diameter$. Due to the fact that one of structural properties have a dimension at the nm scale the fillers are termed nanofillers. Compared with CB these high aspect ratio fillers are know to produce high performance nanocomposites at lower weight fractions [3], being one of the main routes to increase the electrical properties of a polymer material.

The studied fillers in this thesis are high aspect ratio carbon allotropes, namely CNT and VGCNF. Generally the differences between the physical properties of the matrix and the nanofillers is high. For the electrical properties this difference can be of several orders of magnitude. This high contrast in the physical properties of matrix and nanofillers enables the production of nanocomposites with tailored properties for specific applications.

Historically, CNT have their first appearance fifty years ago as undesirable by-products of the fuel coke industry [4]. The subsequent detailed characterization presented in the seminal work of Iijima [5] instigated the attention that has been devoted to the study of these carbon allotropes [2, 6]. CNT can be considered as cylinders of covalently bonded carbon atoms [2] that, depending

on how the graphene honeycomb network is rolled up, results in a CNT that can be considered metallic or semiconductor. The application range for the CNT is vast and includes, among others, conductive and high-strength composites, energy storage and energy conversion devices [7].

Interestingly, VGCNF share a similar story than CNT: they were also observed two centuries ago [8, 9] as reported in [4] and only recently have been characterized [10]. VGCNF are high aspect ratio carbon allotropes with a stacking morphology of truncated conical graphene layers and a hollow core [10]. Compared to CNT, VGCNF have received less research attention as nanofillers because CNT have better mechanical properties (due to smaller microstructural defects), smaller diameter and lower density than VGCNF. On another hand, because of their availability and relatively low price, VGCNF can be an excellent alternative relative to other carbon allotropes [3]. Also, for electrical applications, VGCNF are competitive fillers with carbon fiber (CF) and CB, owing to the lower loading of VGCNF (when compared to CF and CB) that is required to achieve certain electrical conductivity [3].

The carbon allotrope concentration, aspect ratio, and dispersion are known to affect the material response [11, 12, 13]. The electrical properties are particularly sensitive to the concentration of the high aspect ratio carbon allotropes, which is believed to result from the network of highly conductive carbon allotrope forming preferential pathways for the electrical current to flow through [14].

The focus in the past years has been in statistical models to determine the percolation threshold, the critical point where physical properties strongly change, for the electrical conductivity. The foundation of the latter models is described in a seminal work of Kirkpatrick [15] who studied the transport phenomena in inhomogeneous conductors that exhibit a percolation threshold, focusing on the composite conductivity. More recently, Dalmas *et. al* [16] developed a numerical method for the calculation of the electrical conductivity of carbon nanotube-filled polymer composites. Dalmas *et. al* generated the composite microstructure using splines to simulate the penetrable nanotubes. They created an equivalent resistance network that corresponds to the microstructure and solved it using the finite element method. The later model incorporates tube-tube contact resistance and tube resistance, which are fitted to the model using rather limited experimental values. In another work related to the resistor network model [17] the authors developed a model to retrieve the percolation threshold and the electrical conductivity of carbon nanotubes/polymer materials. The developed model accounts for the van der Wall interactions in the construction of the microstructure and the formation of bundles of nanotubes, the nanotubes being represented by rigid cylinders.

After the construction of the microstructure the authors solve the equivalent resistor network using the SPICE 3 computer program developed at Berkeley University. The later models [16, 17] are rather limited in the sense that number of tube bundles or the resistance contact are empirically fitted through limited experimental data [14]. A more recent and complete work based in the resistance network model is presented by Hu et al [14], where a 3D statistical percolation model is developed to predict the percolation threshold of CNT/polymer composites. The microstructure is built using soft-core cylinders using a Monte Carlo algorithm.

The model uses segments with defined angles for the orientation to construct the CNT. The authors also assume that the contact resistance is zero. After the microstructure is formed the authors calculate the electrical conductivity using the matrix representation for a resistor network [15]. The latter models are applicable at the percolation threshold and beyond, and are used to study the conductivity of the composite. Interestingly, there are few numerical models able to explain the effect of adding conductive fillers to a lossless dielectric matrix on the composite dielectric constant. One of the first works was presented by Flandin [18]. The latter authors calculated the electrical conductivity and dielectric permittivity using a network composed by resistors and capacitors (RC). The model uses two parameters, which are fitted trough the model using their own experimental result, namely the composite relative permittivity and electrical conductivity. The experimental values are plugged into the model using the local definition of resistance and conductivity. The later parameters in conjugation with the Kirchhoff current laws, considering only 16 neighbors, gives strikingly good results when compared to the experimental values. The authors were one of the pioneers in using the RC model to explain the composites electric behavior. A more recent work by Simoes *et. al* [19] demonstrates that the dielectric constant increase due to the addition of CNT can be explained by the formation of a capacitor network.

From this description it should be obvious that there is insufficient understanding of the effect of the filler AR and orientation on the composite conductivity and dielectric constant of nanocomposites. There are also some important questions regarding the composite conduction mechanisms.

1.1 Objectives

The major challenges in tailoring nanocomposites are related to controlling the structure and morphology development at the nanoscale, such as the filler dispersion, alignment and aspect ratio. Carbonaceous fillers such as VGCNF and CNT embedded in a polymeric matrix have a wide range of applications, such

as sensors, self-healing materials, electrical shielding, and capacitors. In industry, there is considerable interest in better understanding structure-properties relations for these composites.

The objectives for this thesis are to study the dielectric constant and electrical conductivity of a polymeric composite with embedded high aspect ratio fillers, mainly the influence of the aspect ratio, filler concentration and orientation. It is also an objective of this thesis to increase the understanding of the physical mechanism and phenomena involved in the conduction percolation transition.

1.2 Structure and methodology

This thesis is divided in seven chapters. The first chapter presents an introduction with a succinct review of the state of the art. The results, including a state of the art specifically related to the presented work are presented in chapters two to six and are based in the published paper given in references [20, 21, 22, 23, 24, 25]. In chapter six it is presented an application of the developed methodologies to two experimental cases. Finally the conclusions are presented in chapter seven.

This work starts with a review which is focused in the major problems of the electrostatic response of polymer materials embedded with VGCNF or CNT, i.e, high aspect ratio fillers. The dielectric properties of a polymeric composite where the reinforcements are conductive high aspect ratio fillers is discussed in chapter two. The influence of high aspect ratio fillers embedded in a polymer on the composite conductivity is presented in chapter three. In the following chapter, chapter four, a model based in the network theory is proposed to explain the conductivity of polymers reinforced with high aspect ratio carbon allotrope. The latter model is then applied to two different composites system as presented in chapter six. In chapter five it is explored critical behaviour of a 3D ensemble of high aspect ratio rods.

In this thesis it was developed a software, written in C++, for the generation of the composites materials. It was also built a software, written in C++, for the calculation of of the conductivity. The developed softwares were built using an object oriented approach and the MPI was used for the parallelization of the codes. The codes were run in the SEARCH cluster at the University of Minho.

1.3 References

[1] E. T. Thostenson, C. Li, T.-W. Chou, Nanocomposites in context, Composites Science and Technology 65 (2005) 491.

[2] M. Moniruzzaman, K. I. Winey, Polymer Nanocomposites Containing Carbon Nanotubes, Macromolecules 39 (2006) 5194.

[3] M. H. Al-Saleha, U. Sundarara, A review of vapor grown carbon nanofiber/polymer conductive composites, Carbon 47 (2009) 2.

[4] M. Monthioux, Filling single-wall carbon nanotubes, Carbon 40 (2002) 1809.

[5] S. Iijima, Helical microtubles of graphitic carbon, Nature 354 (1991) 56.

[6] J.-C. Charlier, X. Blase, S. Roche, Electronic and transport properties of nanotubes, Reviews of Modern Physics 79 (2007) 677.

[7] R. H. Baughman, A. A. Zakhidov, W. A. de Heer, Carbon nanotubes–the route toward applications., Science 297 (2002) 787.

[8] P. Schutzenberger, L. Schutzenberger, Sur quelques faits relatifs a 'l'histoire du carbone, Acadimie des Sciences Paris 111 (1890) 774.

[9] C. Pélabon, H. Pélabon, Sur une variété de carbone filamenteux, Acadmie des Sciences Paris 137 (1903) 706.

[10] M. Endo, Y. a. Kim, T. Hayashi, Y. Fukai, K. Oshida, M. Terrones, T. Yanagisawa, S. Higaki, M. S. Dresselhaus, Structural characterization of cup-stacked-type nanofibers with an entirely hollow core, Applied Physics Letters 80 (2002) 1267.

[11] P. Cardoso, J. Silva, M. C. a. Paiva, F. V. Hattum, S. Lanceros-Mendez, Comparative analyses of the electrical properties and dispersion level of VGCNF and MWCNT: Epoxy composites, Journal of Polymer Science Part B: Polymer Physics 50 (2012) 1253.

[12] P. Cardoso, J. Silva, D. Klosterman, J. A. Covas, F. W. J. V. Hattum, R. Simoes, The influence of the dispersion method on the electrical properties of vapor-grown carbon nanofiber / epoxy composites, Nanoscale Research Letters 6 (2011) 370.

[13] P. Pötschke, A. R. Bhattacharyya, A. Janke, Carbon nanotube-filled polycarbonate composites produced by melt mixing and their use in blends with polyethylene, Carbon 42 (2004) 965.

[14] N. Hu, Z. Masuda, Y. Cheng, G. Yamamoto, The electrical properties of polymer nanocomposites with carbon nanotube fillers, Nanotechnology 19 (2008) 215701.

[15] S. Kirkpatrick, Percolation and Conduction, Reviews of Modern Physics 45 (1973) 574.

[16] F. Dalmas, R. Dendievel, L. Chazeau, J.-Y. Cavaille, C. Gauthier, Carbon nanotube-filled polymer composites. Numerical simulation of electrical conductivity in three-dimensional entangled fibrous networks, Acta Materialia 54 (2006) 2923.

[17] M. Grujicic, G. Cao, W. N. Roy, A computational analysis of the percolation threshold and the electrical conductivity of carbon nanotubes filled polymeric materials, Journal of Materials Science 39 (2004) 4441.

[18] L. Flandin, M. Verdier, B. Boutherin, Y. Brechet, J.-Y. Cavaillé, A 3-D numerical simulation of AC electrical properties of short fiber composites, Journal of Polymer Science Part B: Polymer Physics 37 (1999) 805.

[19] R. Simoes, J. Silva, R. Vaia, V. Sencadas, P. Costa, J. Gomes, S. Lanceros-Mendez, Low percolation transitions in carbon nanotube networks dispersed in a polymer matrix: dielectric properties, simulations and experiments, Nanotechnology 20 (2009) 35703.

[20] R. Simoes, J. Silva, S. Lanceros-Mendez, R. Vaia, Influence of fiber aspect ratio and orientation on the dielectric properties of polymer-based nanocomposites, Journal of Materials Science 45 (2009) 268.

[21] J. Silva, S. Ribeiro, S. Lanceros-Mendez, R. Simões, The influence of matrix mediated hopping conductivity, filler concentration, aspect ratio and orientation on the electrical response of carbon nanotube/polymer nanocomposites, Composites Science and Technology 71 (2011) 643–646.

[22] J. Silva, R. Simoes, S. Lanceros-Mendez, R. Vaia, Applying complex network theory to the understanding of high aspect ratio carbon filled composites, Europhysics Letters (EPL) 93 (2011) 37005.

[23] J. Silva, R. Simoes, S. Lanceros-Mendez, Critical behavior of a three-dimensional hardcore-cylinder composite system, Physical Review E 85 (2012) 021115.

[24] P. Cardoso, J. Silva, D. Klosterman, J. A. Covas, F. W. J. V. Hattum, R. Simoes, S. Lanceros-mendez, The role of disorder on the AC and DC

electrical conductivity of vapour grown carbon nanofibre / epoxy composites, Composites Science and Technology 72 (2012) 243–247.

[25] S. A. C. Carabineiro, M. F. R. Pereira, J. Nunes-Pereira, J. Silva, C. Caparros, V. Sencadas, S. Lanceros-Méndez, The effect of nanotube surface oxidation on the electrical properties of multiwall carbon nanotube/poly(vinylidene fluoride) composites, Journal of Materials Science 47 (2012) 8103.

2

Influence of fiber aspect ratio and orientation on the dielectric properties of polymer-based nanocomposites

The addition of conducting fillers to polymeric matrices can significantly improve their electrical properties. Although heterogeneous composites have been widely investigated, the case of nanocomposites containing conductive fillers is not sufficiently understood. In this chapter, the influence of fiber aspect ratio and orientation on dielectric properties of nanocomposites was studied by computer simulation. Simulation results are discussed and related to experimental results. It is confirmed that increasing filler aspect ratio increases the dielectric constant for the same volume fraction. It is also shown that nematic sate composites show a lower dielectric constant when compared to isotropic ones. Finally it is demonstrated that for nematic state materials with different aspect ratios the dielectric constant follows a power law relative to the concentration. This chapter is based on [1].

2.1 Introduction

The addition of carbon nanotubes to a polymeric matrix affects its mechanical and electrical properties. The changes can be significant even at small volume fractions of the reinforcement. The electrical properties are particularly sensitive to the CNT concentration. It is believed that the origin of this effect is the formation of a network of highly conductive CNTs forming preferential pathways for the electrical current to flow through. The CNT concentration, aspect ratio and dispersion are expected to affect the material response [2, 3]. Because of the complexity of the problem and the lack of fundamental understanding on the underlying phenomena, computer simulations can provide useful insights. The focus in the past years has been on statistical models to determine the percolation threshold. The percolation threshold or the concentration where an infinite cluster appears [4] can be predicted for high aspect

ratio fillers in the framework of the excluded volume theory. In general, the percolation threshold is defined within the following bounds:

$$1 - e^{-\frac{1.4V}{\langle V_e \rangle}} \leq \Phi_c \leq 1 - e^{-\frac{2.8V}{\langle V_e \rangle}} \tag{2.1}$$

Eq. (2.1), links the average excluded volume,$\langle V_e \rangle$,the volume around an object in which the center of another similarly shaped object is not allowed to penetrate averaged over the orientation distribution and the critical concentration (Φ_c). Here, the value 1.4 corresponds to the lower limit infinitely thin cylinders and the value 2.8 corresponds to spheres. The derivation of this equation and related discussion has been presented in [5]. With respect to the percolation threshold of high aspect ratio fillers it is also worth to mention the statistical work of Munson-McGee [6]. Berhan et al. [7, 8] also studied the percolation threshold of high aspect ratio fillers using soft core and hard core models. They draw two important conclusions that gave further confidence to the applicability of the excluded volume concept: that the hard-core approach is more appropriate for modeling electrical percolation onset in nanotube-reinforced composites and other high-aspect-ratio fiber systems, and that for high aspect-ratio fibers, the generally accepted inverse proportionality between percolation threshold and excluded volume holds, independent of fiber waviness. The influence of the aspect ratio on the electrical properties of nanocomposites has been addressed in a recent experimental article by Sheng-Hong et al. [9]. They studied the electrical properties of MWCNT/PVDF composites. It was found that increasing aspect ratio increases the dielectric constant and the percolation threshold of the composite. The increase of the percolation threshold with the aspect ratio deviates from the predictions using the excluded volume theory. These authors explained this deviation with the formation of agglomerates which reduced the fillers effective aspect ratio, increasing the percolation threshold. The increase of the dielectric constant with filler volume fraction can be understood within the framework of the percolation theory [4] . The behavior of the conductivity and the dielectric constant at the composite critical concentration was studied earlier by Bergman and Imry [10] for heterogeneous mixtures of a conducting phase and an insulating matrix. An important result in this work is the divergence at the percolation threshold. The theoretical prediction was later completed in subsequent works by Stroud and Bergman [11]. A recent review in carbon fiber composites also addresses the problem of the wide range of critical concentrations values for the same type of filler/polymer composites [12] and the critical exponent s. The effect of the alignment on the conductivity has been studied both numerically [13] and experimentally [14]. Experimental and numerical results demonstrate that as the anisotropy increases, for a fixed concentration, there

is a critical value for the axial orientation parameter ($S = (3\langle\cos^2\theta\rangle - 1) * 0.5$, where S varies from 0 to 1 for isotropically and anisotropically oriented fibers, respectively. The same authors also observed a critical value for the axial orientation parameter (S_c) and, after that, a decrease in the conductivity. In our previous work [15], a numerical procedure was developed enabling the calculation of the composite dielectric constant, dielectric strength and voltage breakdown. The numerical results have been validated against experimental results. In yet earlier work, it was employed molecular dynamics simulations to study the structure-properties relationships driving the mechanical properties of polymer-based materials [16, 17]. That work included analysis of the true stress development in amorphous polymers, and the effect of loading conditions on deformation and creep. In this chapter it is discussed the influence of the aspect ratio and the orientation of the nanotubes on the dielectric constant of polymer nanocomposites. In order to do this, isotropic and nematic materials were generated.

2.2 Methods

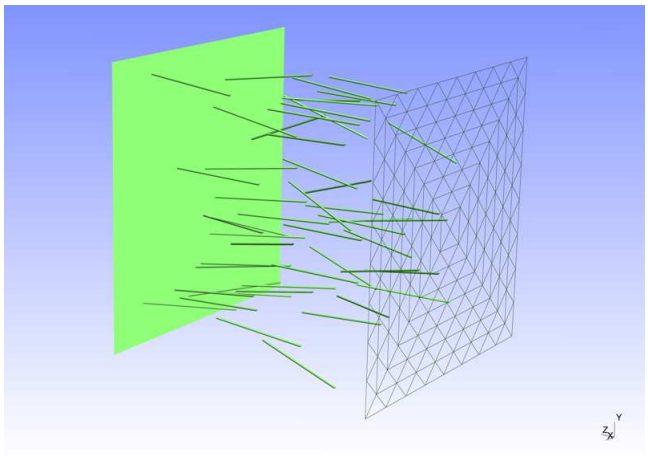

Figure 2.1: Representation of a nematic material with an aspect ratio of 50

As described in [15] , the microstructure is generated by placing randomly oriented cylinders with an aspect ratio of fifty and ten with a derivation of a sequential packing algorithm [18] for the isotropic materials. For the nematic state materials it was constrained the zenith angle between 0° and 20° and randomly place the cylinders in domains; see Fig. 2.1. A minimum separation threshold of 1.0 nm was also defined with the purpose of avoiding quantum tunnelling effects. The threshold value is based on predictions of the order

of the tunneling distance as 1 nm [19]. For each concentration, ten different materials were generated with the same basic parameters, and then their final properties averaged. The properties of the dielectric matrix were kept constant in all cases; a dielectric constant value of 7 was chosen, from that of $\alpha - PVDF$. The model was tested for consistency, proving that the values of the dielectric constant are independent of the number of particles in the box. For example, calculations for $\Phi = 5E-3$ in the cases of $N = 66$ and $N = 100$, revealed 16% deviation on average.

2.3 Results and discussion

In Fig. 2.2 the results for the dielectric constant of random and nematic materials are shown. From the error bars, it is concluded that the standard error is higher for the random materials.

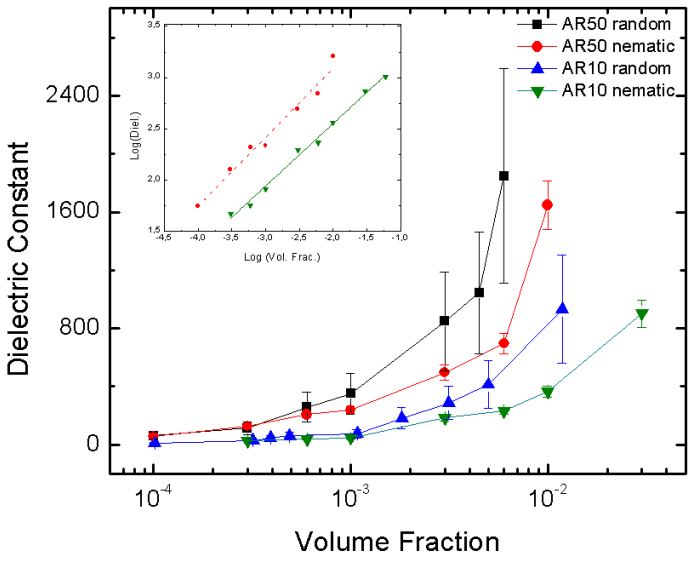

Figure 2.2: Results for random and nematic materials with different aspect ratios (AR 10 and AR 50). In the inset the log-log plot for the nematic materials.

This is related to the effect of the minimum distance and the rotation angle on the local capacitance [15] . For the anisotropic materials, a decrease of the standard error is observed due to the orientation of the cylinders. Also, based in Fig. 2.2, it can be concluded that: a) increasing the aspect ratio will increase the dielectric constant (in agreement with recent experimental results for the MWCNT/PVDF composites [9]; b) nematic materials have a lower dielectric

constant compared to isotropic ones. This result supports the ones previously obtained for the electrical conductivity [14].

The fact that nematic materials show a lower dielectric constant than isotropic ones (Fig. 2.2) is related to the zenith angle. It was demonstrated in [15] that parallel cylinders exhibit a lower capacitance, so the lower value for the composite dielectric constant is related to the filler alignment. It should be noted that in our simulations all the fillers are interacting with each other, removing the effect of different network topologies on the results, i.e., the number of serial or parallel capacitors in the network is the same for each material. Using the results in Fig. 2.2 a power law can be fitted for the two nematic materials (AR 10 and AR 50). For the nematic AR 50 material, a linear fit in a log log plot has a slope of 0.67 ± 0.48 and an intercept value of 4.43 ± 0.15. For the nematic AR 10 materials the slope is 0.61 ± 0.48 and the intercept 3.77 ± 0.56. The adjusted R-square for nematic AR 50 and AR 10 were 0.97 and 0.99. The later values indicate that the dielectric constant follows a power law:

$$\varepsilon(\Phi) = a\Phi^b \tag{2.2}$$

In Fig. 2.2 (inset), the log-log plots for the two types of nematic materials are shown.The b exponent should ideally have a lower deviation in order for us to try to relate the b values to physical features of the material, such as the dispersion. In any case, the b exponent values found for the two ARs are fairly similar excluding any relation with the filler aspect ratio. The obtained power laws (Eq. (2.2)) for the dielectric constant can be compared to similar ones previously obtained by Hu et al. [19] for the conductivity (Eq. (16) in the later article). Hu et al. [20] included a dependence on the aspect ratio in the percolation equation for straight CNTs, namely in the scaling constant. From the power laws calculated from our results, it can be seen that the a constant for AR 10 is 4.56 times greater than that of AR 50 one, so the a constant is related with filler aspect ratio, supporting the results of [20], in the limit of $\Phi_c \to 0$. Also by dividing the a constant by a suitable factor we can empirically find the results for lower AR using the calculated power laws.

This type of behavior, the continuous increase of the dielectric constant, is observed in several experimental results [21, 22, 23] and is related to the formation of a capacitive network where the long range Columbic interactions prevail [15]. Similar trends have also been found in related experimental work for MWCNT/PVDF composites [24].

2.4 Conclusion

In summary, it was found that an increase of the aspect ratio of the fillers increases the dielectric constant of the nanocomposite for the same volume fraction supporting recent experimental results for the dielectric constant in nanocomposites [9]. The nematic materials show a lower dielectric constant compared to isotropic ones the same behaviour had previously been found experimentally for the electrical conductivity [14]. It was also demonstrated that for nematic state materials with different aspect ratios, the dielectric constant follows a power law. The difference in the aspect ratios is reproduced in the power law scaling constant. Also, the power law exponent remains unchanged suggesting that it is related with the filler distribution and degree of anisotropy.

2.5 References

[1] R. Simoes, J. Silva, S. Lanceros-Mendez, R. Vaia, Influence of fiber aspect ratio and orientation on the dielectric properties of polymer-based nanocomposites, Journal of Materials Science 45 (2009) 268.

[2] E. T. Thostenson, C. Li, T.-W. Chou, Nanocomposites in context, Composites Science and Technology 65 (2005) 491.

[3] M. Moniruzzaman, K. I. Winey, Polymer Nanocomposites Containing Carbon Nanotubes, Macromolecules 39 (2006) 5194.

[4] D. Stauffer, A. Aharony, Introduction to Percolation Theory, Taylor and Francis, London, 1992.

[5] A. Celzard, E. McRae, C. Deleuze, M. Dufort, G. Furdin, J. F. Marêché, Critical concentration in percolating systems containing a high-aspect-ratio filler, Physical Review B 53 (1996) 6209.

[6] S. H. Munson-McGee, Estimation of the critical concentration in an anisotropic percolation network, Physical Review B 43 (1991) 3331.

[7] L. Berhan, A. M. Sastry, Modeling percolation in high-aspect-ratio fiber systems. I. Soft-core versus hard-core models, Physical Review E 75 (2007) 41120.

[8] L. Berhan, A. M. Sastry, Modeling percolation in high-aspect-ratio fiber systems. II. The effect of waviness on the percolation onset, Physical Review E 75 (2007) 41121.

[9] S.-H. Yao, Z.-M. Dang, M.-J. Jiang, H.-P. Xu, J. Bai, Influence of aspect ratio of carbon nanotube on percolation threshold in ferroelectric polymer nanocomposite, Applied Physics Letters 91 (2007) 212901.

[10] D. J. Bergman, Y. Imry, Critical Behavior of the Complex Dielectric Constant near the Percolation Threshold of a Heterogeneous Material, Physical Review Letters 39 (1977) 1222.

[11] D. Stroud, D. J. Bergman, Frequency dependence of the polarization catastrophe at a metal-insulator transition and related problems, Physical Review B 25 (1982) 2061.

[12] M. H. Al-Saleha, U. Sundarara, A review of vapor grown carbon nanofiber/polymer conductive composites, Carbon 47 (2009) 2.

[13] S. I. White, B. A. DiDonna, M. Mu, T. C. Lubensky, K. I. Winey, Simulations and electrical conductivity of percolated networks of finite rods with various degrees of axial alignment, Physical Review B 79 (2009) 24301.

[14] F. Du, J. Fischer, K. Winey, Effect of nanotube alignment on percolation conductivity in carbon nanotube/polymer composites, Physical Review B 72 (2005) 121404.

[15] R. Simoes, J. Silva, R. Vaia, V. Sencadas, P. Costa, J. Gomes, S. Lanceros-Mendez, Low percolation transitions in carbon nanotube networks dispersed in a polymer matrix: dielectric properties, simulations and experiments, Nanotechnology 20 (2009) 35703.

[16] R. Simoes, A. M. Cunha, W. Brostow, Molecular dynamics simulations of polymer viscoelasticity: effect of the loading conditions and creep behaviour, Modelling and Simulation in Materials Science and Engineering (2006) 157.

[17] R. Simões, A. M. Cunha, W. Brostow, Computer simulations of true stress development and viscoelastic behavior in amorphous polymeric materials, Computational Materials Science 36 (2006) 319.

[18] M. J. Vold, Sediment Volume and Structure in Dispersions of Anisometric Particles, The Journal of Physical Chemistry 63 (1959) 1608.

[19] I. Balberg, Tunneling and nonuniversal conductivity in composite materials, Physical Review Letters 59 (1987) 1305.

[20] N. Hu, Z. Masuda, Y. Cheng, G. Yamamoto, The electrical properties of polymer nanocomposites with carbon nanotube fillers, Nanotechnology 19 (2008) 215701.

[21] A. Mdarhri, F. Carmona, C. Brosseau, P. Delhaes, Direct current electrical and microwave properties of polymer-multiwalled carbon nanotubes composites, Journal of Applied Physics 103 (2008) 54303.

[22] K. Ahmad, W. Pan, S.-L. Shi, Electrical conductivity and dielectric properties of multiwalled carbon nanotube and alumina composites, Applied Physics Letters 89 (2006) 133122.

[23] B.-K. Zhu, S.-H. Xie, Z.-K. Xu, Y.-Y. Xu, Preparation and properties of the polyimide/multi-walled carbon nanotubes (MWNTs) nanocomposites, Composites Science and Technology 66 (2006) 548.

[24] Z.-M. Dang, L. Wang, Y. Yin, Q. Zhang, Q.-Q. Lei, Giant Dielectric Permittivities in Functionalized Carbon-Nanotube/ Electroactive-Polymer Nanocomposites, Advanced Materials 19 (2007) 852.

3

The influence of matrix mediated hopping conductivity, filler concentration, aspect ratio and orientation on the electrical response of carbon nanotube/polymer nanocomposites

A model to simulate the conductivity of carbon nanotube/polymer nanocomposites is presented. The proposed model is based on hopping between the fillers. A parameter related to the influence of the matrix in the overall composite conductivity is defined. It is demonstrated that increasing the aspect ratio of the fillers will increase the electrical conductivity. It is also shown that anisotropic composites show lower values for the conductivity than isotropic ones. Finally, it is demonstrated that the alignment of the filler rods parallel to the measurement direction results in higher conductivity values, in agreement with results from recent experimental works. This chapter is based on [1].

3.1 Introduction

One attempt to increase the application range of polymers is through the incorporation of nanoscale fillers with intrinsically high electrical conductivity into the polymeric matrix. Among nanoscale modifiers, carbon nanotubes (CNT) present high electric conductivity ($10^3 - 10^4$ S/cm) and tensile strength [2]. These facts, together to the relatively easy incorporation and dispersion into polymers, raised the interest in CNT to provide solutions to some problems in composite applications [3]. In order to be used in tailored composite applications, the conduction mechanism must be understood. The composite conductivity is generally described by the percolation theory [4], predicting a power law relation:

$$\sigma \sim \sigma_0 \left(\Phi - \Phi_c\right)^t, \text{ for } \Phi > \Phi_c \tag{3.1}$$

where t is a universal critical exponent that depends only on the system dimension, Φ is the volume fraction and Φ_c is the critical concentration at

which an infinite cluster appears. For $\Phi > \Phi_c$, a cluster spans the system, whereas for $\Phi < \Phi_c$ the spanning cluster does not exist and the system is comprised of many small clusters. Interestingly, the predictions of the percolation theory and the excluded volume theory are not verified for CNT/polymer composites, as can be seen in recent reviews [5, 2]. In addition to studies on the percolation and excluded volume theory, several authors tried to cope with the effect of the volume fraction, clustering and anisotropy in the conductivity of CNT/polymer composites. In this section, the most relevant studies to our own work will be reviewed. Dalmas *et. al* [6] modelled the conductivity in 3D fibrous networks using soft-core cylinders. They studied the effect of fibre tortuosity and fibre-fibre contact conductivity in the composite electric conductivity. It was found a good agreement between simulation and experimental results with one adjustable parameter, the fibre tortuosity. The existence of contact conductivity was also proposed by Hu *et. al* [7] using soft-core cylinders. The influence of aspect ratio, electrical conductivity, aggregation and shape of CNT in the composite electric conductivity was also studied. It was found, similarly to Dalmas *et. al* [6], that the percolation threshold increases with the fibre tortuosity. Nonetheless, the fibre tortuosity has a limited effect on the global composite conductivity. In addition, Hu *et. al* [7] found that the aggregation has a significant effect on the composite conductivity: the composite conductivity decreasing with increasing aggregation. The contact resistivity was also investigated by Sun *et. al* [8] in a continuum model. The authors conclude that the contact and tunnelling resistance must be controlled in order to achieve high conductive CNT/polymer composites. Finally White *et. al* [9] investigated the effect of CNT orientation using soft-core cylinders. It was found that there is a critical degree of orientation above which the electrical conductivity decreases. In a previous paper [10], we demonstrated that CNT/epoxy conductivity can be described by a single tunnel junction expression [11]$\sigma_{DC} = \sigma_0 e^{(-2\chi_T d)}$, where $\chi_T = \sqrt{\frac{2mV(T)}{h^2}}$, m represents the mass of the charge carriers, d the barrier width and $V(T)$ the temperature modified barrier height [12]. In the present work, it is shown that hopping mediated by the polymer matrix can explain the conductivity of these composites. In this way, a new model, based on hard-core cylinders with no contact resistance, is proposed.

3.2 Methods

The influence of the matrix mediated hopping conductivity on the composite conductivity for different values of the aspect ratio and filler orientation was studied. For isotropic composites, fibers are initially positioned in 3D space

with a derivation of a sequential packing algorithm [13, 14, 15]. In this process, a cylinder position is accepted if the minimum distance to any other cylinder is larger than the cylinder diameter; otherwise, the position is rejected and a new one is tested until it can be placed. This process is repeated until the desired volume fraction is achieved. Once the generation of the composite is completed, a resistor network is extracted by assigning a resistor between two rods that are at a minimum distance lower than some threshold, δ_{max}, the maximum value for the minimum separation distance. To complete the process we extract the list of connected bonds using the depth-first search algorithm [16]. After the generation of the microstructure, the conductivity can be found using the matrix representation for a resistor network and the Kirchhoffs current laws [17]. More precisely, the linear system is solved using the incomplete Cholesky conjugated gradient method. A range of volume fractions were generated in a cube of side 25000 nm for isotropic cases corresponding to a range of $\sim$ 800 to 14000 cylinders with length 5000 nm and a diameter value that depends on the aspect ratio. Five different materials were evaluated and an error of 5% was determined. For the anisotropic study, the axial orientation parameter is initially defined as:

$$S = \frac{\left(3\langle cos^2\theta\rangle - 1\right)}{2} \tag{3.2}$$

where S varies from -0.5 to 1; 0 for a isotropic composite (Fig. 3.1, left), 1.0 for cylinders with a parallel orientation (Fig. 3.1, right) and -0.5 for cylinders with perpendicular orientation.

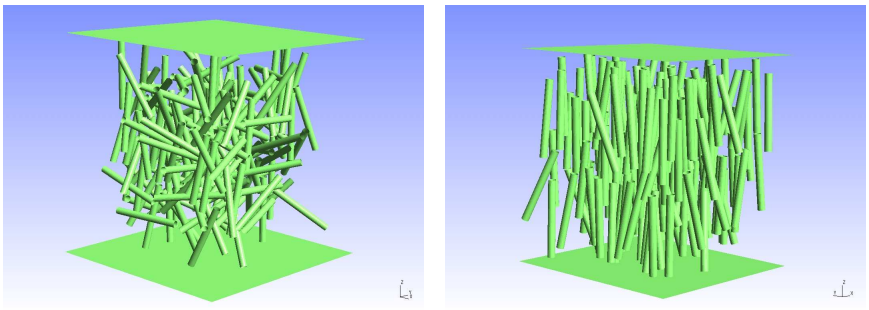

Figure 3.1: Representation of an isotropic virtual material (left) and an anisotropic material (right). For all simulations the domain is larger that the one presented here.

In our case, S=1 corresponds to a composite with cylinders oriented perpendicular to the measurement direction and S=-0.5 to cylinders oriented parallel to the measurement direction. For the anisotropic materials the zenith angle is determined by a Gaussian distribution in $\cos\theta$ and randomly placement of the

cylinders in domains following the previous stated procedure for the isotropic composites. The alignment was evaluated using Eq. (3.2) and a range of volume fractions were generated in a cube of side 25000 nm which corresponds to ~ 800 to 10000 cylinders with length of 5000 nm and a diameter of 50 nm. It has been previously demonstrated that the conductance of CNT/polymer composites can be explained by a transition from a strong disorder regime into a weak disorder one [18]. With the latter in mind, the bonds between two fillers have an assigned conductance defined as:

$$G = G_0 e^{-a[0,1]} \tag{3.3}$$

where G_0 is the filler conductance for metallic armchair CNT having the value of $4e^2h$ [19], with e being the electron charge, h the Planck constant, a a constant that controls the disorder strength and $[0, 1]$ the interval of a uniform distribution between 0 and 1. Eq. (3.3) is similar to the expression of Miller *et. al* [20] for hopping at room temperature:$\sigma_{ij} = \sigma_0 e^{-\frac{x_{ij}}{x_0}}$, where x_{ij} is the distance between two fillers in our case the minimum distance between two rods; x_0 is the scale over which the wave function decays in the matrix and 0 the dimension coefficient. Also in [18], the following relation is obtained for isotropic composites:

$$\Phi_c = \frac{D^2}{2\delta_{max} L} \tag{3.4}$$

where D is the fiber diameter, L the fiber length and δ_{max} the maximum value for the rod minimum separation distance related to the conduction mechanism: hopping. Eq. (3.4) is similar to the one obtained in [21].The disorder constant äïs related to δ_{max} [18] and in this work we restrain ourselves to the weak disorder regime. This regime has already been observed experimentally [10, 18, 22] and can be described by the following linear relation: $log\,(\sigma) \sim \phi^{-\frac{1}{3}}$ [18]. For that, we set $\delta_{max} = \xi$, with ξ being the correlation length that depends on the length of the optimal path between two fillers [18]. Resulting in äv̈alue close to the unit, meaning, in the weak disorder regime where all bonds contribute to the conductivity.

3.3 Results and discussion

The conductivity for different aspect ratio is presented in Fig. 3.2: The conductivity increases with increasing aspect ratio.

Applying the power law (Fig. 3.2 inset) defined by the percolation theory, Eq. (3.1) with Eq. (3.4), results in $t \sim 1.0$ with $R^2 \sim 0,97$ for all fits. The latter value for the critical exponent is equal to that predicted by the

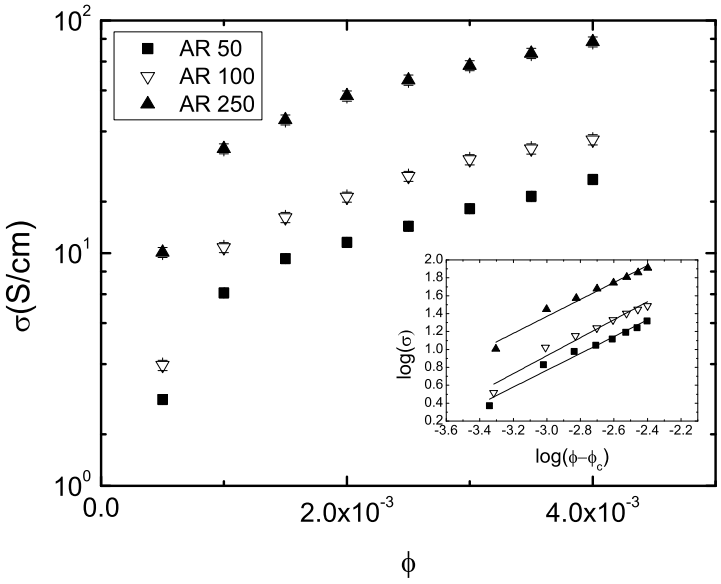

Figure 3.2: Conductivity versus volume fraction for three different aspect ratios.Inset log-log plot and linear fit with Eq. (3.1) and the critical volume fraction given by Eq. (3.4).

effective medium theory [17] . The observed increase of the conductivity with the aspect ratio is in agreement with [7] and can be explain by a decrease in the percolation threshold for increasing filler aspect ratio. It should be noted that in our simulations the conductance of the cylinder (CNT) is independent of the filler length, contrary to [6, 7, 8]. Furthermore, as the present model does not assume a contact resistance, the composite conductivity results only from the CNT with max controlling the hopping length for the same aspect ratio. In this way, δ_{max} is a parameter that can be associated to the dielectric matrix, i. e., different types of polymer will correspond to different values of δ_{max}. For instance, in epoxy composites, increasing the postcure temperature will increase the cross-link density [23] increasing the composite conductivity [24]; this can be seen as an increase on the value of δ_{max}. Fig. 3.3 shows that the conductivity increases with δ_{max} for fibers with the same aspect ratio (100).

Increasing δ_{max} will increase the number of fillers that are available to conduction, decreasing the number of bonds to transverse the domain, i.e., decreasing the length of the optimal path [18]. Also, as stated by Eq. (3.4), an increase of δ_{max} will decrease the percolation threshold. As stated before, the parameter δ_{max} can be easily related to the cross-link density and hence

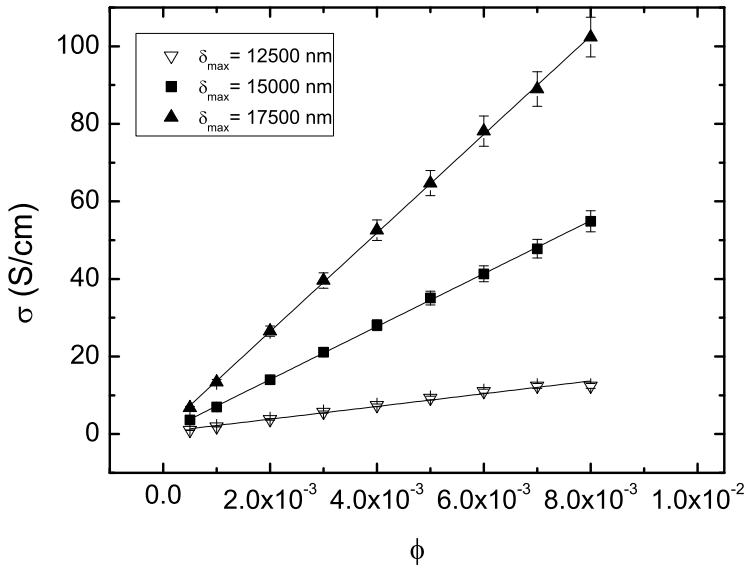

Figure 3.3: Conductivity as a function of the volume fraction for several values of δ_{max}

depends on the nature of the polymeric matrix. Aside from the relation between δ_{max} and the polymer, the latter parameter is linked with the disorder strength (ä) as previously discussed. This disorder constant, ä; can be linked to the inverse of the scale of wave decay in the matrix, as stated by the Miller hopping formula [20]. Therefore,δ_{max} is also related to the conduction mechanism, i. e., hopping mediated by the matrix. In Fig. 3.4 are presented the values of the composite conductivity for different degrees of axial alignment (Eq. (3.2)) and different volume fractions.

A decrease in the conductivity for the more anisotropic composites can be observed, with this effect being more prominent at higher volume fractions. Comparing to the results in [9], a critical value for the axial alignment is not observed, but only a decrease in conductivity. This decrease in conductivity can be explained by an increase of the number of fillers that is necessary to transverse the domain between the applied electrodes. Increasing the number of fillers will increase the number of resistors and hence decrease the conductivity. Thus, increasing anisotropy changes the conductivity to lower values due to a higher number of fillers that are necessary to transverse the domain. Furthermore, as the number of fillers in the domain increases by increasing the volume fraction the difference between isotropic and anisotropic composite conductivity will be larger. Fig. 3.4 also shows that there is a substantial

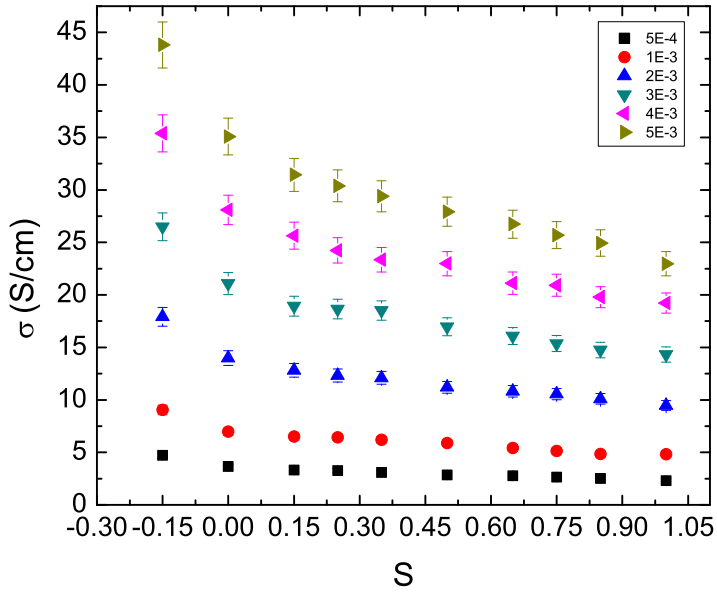

Figure 3.4: Conductivity as a function of the axial alignment (S).

difference in the conductivity between cylinders aligned perpendicular ($S = 1$) and parallel ($S = -0.5$) to the measurement direction. This difference in the conductivity is in agreement to recent experimental work [25] and is explained by the higher number of fillers necessary to transverse the domain ($S = 1$).

3.4 Conclusion

It is demonstrated that simulations based on hard-core cylinders can describe the conductivity of CTN/polymer nanocomposites. The simulations demonstrate that increasing aspect ratio will increase conductivity. On the other hand, increasing the anisotropy will decrease conductivity; this effect is more evident at higher volume fractions. Finally, it is demonstrated that the alignment of rods parallel to the measurement direction results in higher conductivity values, in agreement to recent experimental work.

3.5 References

[1] J. Silva, S. Ribeiro, S. Lanceros-Mendez, R. Simões, The influence of matrix mediated hopping conductivity, filler concentration, aspect ratio

and orientation on the electrical response of carbon nanotube/polymer nanocomposites, Composites Science and Technology 71 (2011) 643–646.

[2] M. H. Al-Saleha, U. Sundarara, A review of vapor grown carbon nanofiber/polymer conductive composites, Carbon 47 (2009) 2.

[3] E. T. Thostenson, C. Li, T.-W. Chou, Nanocomposites in context, Composites Science and Technology 65 (2005) 491.

[4] D. Stauffer, A. Aharony, Introduction to Percolation Theory, Taylor and Francis, London, 1992.

[5] W. Bauhofer, J. Z. Kovacs, A review and analysis of electrical percolation in carbon nanotube polymer composites, Composites Science and Technology 69 (2009) 1486.

[6] F. Dalmas, R. Dendievel, L. Chazeau, J.-Y. Cavaille, C. Gauthier, Carbon nanotube-filled polymer composites. Numerical simulation of electrical conductivity in three-dimensional entangled fibrous networks, Acta Materialia 54 (2006) 2923.

[7] N. Hu, Z. Masuda, Y. Cheng, G. Yamamoto, The electrical properties of polymer nanocomposites with carbon nanotube fillers, Nanotechnology 19 (2008) 215701.

[8] X. Sun, M. Song, Highly Conductive Carbon Nanotube/Polymer Nanocomposites Achievable?, Macromolecular Theory and Simulations 18 (2009) 155.

[9] S. I. White, B. A. DiDonna, M. Mu, T. C. Lubensky, K. I. Winey, Simulations and electrical conductivity of percolated networks of finite rods with various degrees of axial alignment, Physical Review B 79 (2009) 24301.

[10] P. Cardoso, J. Silva, A. J. Paleo, F. W. J. van Hattum, R. Simões, S. Lanceros-Mendez, The dominant role of tunneling in the conductivity of carbon nanofiber-epoxy composites, Physica Status Solidi A 207 (2009) 407.

[11] T. A. Ezquerra, M. Kulescza, F. J. Baltá-Calleja, Electrical transport in polyethylene-graphite composite materials, Synthetic Metals 41 (1991) 915.

[12] H. Kawamoto, E. J. Sichel, Carbon black-polymer composites, Marcel Dekker, New York, 1982.

[13] M. J. Vold, Sediment Volume and Structure in Dispersions of Anisometric Particles, The Journal of Physical Chemistry 63 (1959) 1608.

[14] R. Simoes, J. Silva, S. Lanceros-Mendez, R. Vaia, Influence of fiber aspect ratio and orientation on the dielectric properties of polymer-based nanocomposites, Journal of Materials Science 45 (2009) 268.

[15] R. Simoes, J. Silva, R. Vaia, V. Sencadas, P. Costa, J. Gomes, S. Lanceros-Mendez, Low percolation transitions in carbon nanotube networks dispersed in a polymer matrix: dielectric properties, simulations and experiments, Nanotechnology 20 (2009) 35703.

[16] T. H. Cormen, C. E. Leiserson, R. L. Rivest, C. Stein, Introduction to algorithms, MIT Press, Cambridge, 2001.

[17] S. Kirkpatrick, Percolation and Conduction, Reviews of Modern Physics 45 (1973) 574.

[18] J. Silva, R. Simoes, S. Lanceros-Mendez, R. Vaia, Applying complex network theory to the understanding of high aspect ratio carbon filled composites, Europhysics Letters (EPL) 93 (2011) 37005.

[19] J.-C. Charlier, X. Blase, S. Roche, Electronic and transport properties of nanotubes, Reviews of Modern Physics 79 (2007) 677.

[20] A. Miller, E. Abrahams, Impurity Conduction at Low Concentrations, Physical Review 120 (1960) 745.

[21] A. V. Kyrylyuk, P. van der Schoot, Continuum percolation of carbon nanotubes in polymeric and colloidal media, Proceedings of the National Academy of Sciences 105 (2008) 8221.

[22] A. Allaoui, S. V. Hoa, M. D. Pugh, The electronic transport properties and microstructure of carbon nanofiber/epoxy composites, Composites Science and Technology 68 (2008) 410–416.

[23] I. Irurzun, J. Vicente, M. Cordero, E. Mola, Fractal analysis of electrical trees in a cross-linked synthetic resin, Physical Review E 63 (2000) 016110.

[24] G. Faiella, F. Pscitelli, M. Lavorgna, V. Antonucci, M. Giordano, Tuning the insulator to conductor transition in a multiwalled carbon nanotubes / epoxy composite at substatistical percolation threshold, Applied Physics Letters 95 (2009) 153106.

[25] A. Dombovari, N. Halonen, A. Sapi, M. Szabo, G. Toth, J. Mäklin, K. Kordas, J. Juuti, H. Jantunen, A. Kukovecz, Moderate anisotropy in the electrical conductivity of bulk MWCNT/epoxy composites, Carbon 48 (2010) 1918–1925.

4

Applying complex network theory to the understanding of high-aspect-ratio carbon-filled composites

This work demonstrates that the theoretical framework of complex networks typically used to study systems such as social networks or the World Wide Web can be also applied to material science, allowing deeper understanding of fundamental physical relationships. In particular, through the application of the network theory to carbon nanotubes or vapor grown carbon nanofiber composites, by mapping fillers to vertices and edges to the gap between fillers, the percolation threshold has been predicted and a formula that relates the composite conductance to the network disorder has been obtained. The theoretical arguments are validated by experimental results from the literature. This chapter is based on [1].

4.1 Introduction

The inclusion of high aspect ratio fillers like carbon nanotubes (CNT) or vapour grown carbon nanofibers (VGCNF) in a polymeric matrix enhances the electrical and mechanical properties [2] of the matrix. The filler concentration, aspect ratio (AR), and dispersion are expected to affect the material response [2]. Both for CNT/polymer or VGCNF/polymer composites a divergence in the composite conductivity is expected for a critical volume fraction. This divergence is usually discussed in the framework of the percolation theory [3]. The percolation threshold, or the critical volume fraction, is the concentration at which an infinite cluster appears [3, 4]. It can be predicted for high aspect ratio fillers from the excluded volume theory. In general, the percolation threshold is defined within the following bounds:

$$1 - \exp\left(\frac{-1.4V}{\langle V_{ex}\rangle}\right) \leq \Phi_c \leq 1 - \exp\left(\frac{-2.8V}{\langle V_{ex}\rangle}\right) \tag{4.1}$$

Eq. (4.1) relates the average excluded volume, $\langle V_{ex}\rangle$, the volume around an object in which the center of another similarly shaped object is not allowed

to penetrate, averaged over the orientation distribution, and the critical concentration (Φ_c). Here, the value 1.4 corresponds to infinitely thin cylinders and the value 2.8 corresponds to spheres. The derivation of this equation and related discussion has been presented in [4]. With respect to the percolation threshold of high aspect ratio fillers, it is also worthwhile to mention the statistical work of Munson-McGee [5] and the study of the percolation threshold of soft core and hard core models by Berhan *et. al.* [6, 7]. In a recent review [8] the experimental percolation thresholds for CNT composites revealed the existence of a wide range of values for the same type of CNT/polymer composites, a deviation from the bounds predicted by the excluded volume theory and a dispersion for the values of the critical exponent (t) [3]. The latter exponent is expected to be independent of filler geometry or matrix, taking a value that just depends on the system dimension.

In the past decades, several models have been developed to study network properties. The most relevants to the present work are the random graph models proposed by Erdös and Rény[9] (ER) as seen in [10]. Detailed reviews on the subject can be found in [10]. An important property of random graphs is the existence of a phase transition at the percolation threshold $\langle z \rangle = 1$, where z is the degree for some vertice (the number of first neighbors) and $\langle z \rangle$ is the average degree of the graph. For $\langle z \rangle$ larger than the unit, the size of the largest connected component (giant component, S) is given by [10]:

$$S \sim \exp\left(\langle z \rangle - 1\right)^{\beta} \tag{4.2}$$

In the case of random graphs, the critical exponent $\beta = 1$ in Eq. (4.2)[10]. In the case of random graphs it is also expected that the size of the graph occupied by the giant component obeys the following relation [10]; $S = 1 - \exp\left(-zS\right)$. Finally, in a random graph $\langle z \rangle = \frac{2m}{N}$; where m is the number of edges in the graph and N the number of vertices [11].

By assigning a weight to each edge in the graph, a weighted or disorder network is obtained. The weights in this network indicate the difficulty in traversing the edge: the larger the edge weight, the harder it is to traverse it. If two vertices in the network are considered, an optimal path (ℓ_{opt}) between the two vertices can be defined as the single path for which the sum of the weights along the path is minimum. When most of the links of the path contribute to the sum, the system is said to be "weakly disorder"[12]. On the other hand, the situation in which one link dominates the sum along the path is called the strong disorder limit[12]. The length of the optimal path ℓ_{opt} can be related to the number of vertices in the network, as found by Braunstein *et al*[13] for the strong and weak disorder cases. For the strong disorder case in the ER[9] model $\ell_{opt} \sim N^{\frac{1}{3}}$ and, in the weak disorder case, in the ER[9] model

$\ell_{opt} \sim ln\ N$. Sreenivasan *et al*[12] studied the transition between strong and weak disorder regimes in the scaling properties of the average optimal path in ER[9] and scale free networks. This was performed by assigning to each edge in the network a random number r_i taken from an uniform distribution between 0 and 1. With a weight associated to each edge given by:

$$\tau_i = \exp(ar_i) \tag{4.3}$$

where a represents the strength of the disorder, the case $a \to \infty$ corresponds to the strong disorder limit. With r_1 and r_2 being two random numbers associated with two consecutive links and $r_1 > r_2$, then[12]:

$$\frac{\tau_1}{\tau_2} = \exp(a\Delta r) \tag{4.4}$$

where $\Delta r = r_1 - r_2$. In the strong disorder case $a\Delta r \gg 1$ and the weak disorder limit appears when $a\Delta r \sim 1$, when all links become equivalent.

Advances in materials characterization [14] using conduction-tip atomic force microscopy (CAFM) revealed values for the critical geometrical exponent β. Interestingly, the results suggest that the conductivity network belongs to the same dimension of a Bethe lattice. Some questions were left open by the authors, particularly the high value for the coordination number at the percolation threshold and the influence of cycles on the composite conductivity. The present work is devoted to answering these open questions and to propose a new theoretical framework for the observed conductivity in these composites. First, it will be demonstrated making use of computer simulations, that the complex network framework is suitable for the study of CNT/polymer or VGCNF/polymer composites. It is explained the latter results and further show that the conduction in VGCNF/polymer composites can be described by a Bethe Lattice and that the conductance can be related to a weak disorder limit. Finally,an equation is proposed for the percolation threshold and for the composite conductance obtained within the framework of the complex network theory.

4.2 Methods

In order to study the microstructures found in CNF/polymer nanocomposites, we start by representing those structures on the computer. With computer simulations, we can control in detail the material morphology, nanofiber content, nanofiber orientation, and many other material features[15]. The microstructure for isotropic materials is generated using a derivation of a sequential packing algorithm [16] to place randomly oriented cylinders in 3D space. After

creating the virtual composite, the graph theory framework was used to study the composite's percolation threshold. Within this framework, the cylinders are mapped to vertices and the edges to the minimum distance between the cylinders, which corresponds to the maximum electric field between the two fillers [17]. A maximum value for the minimum separation distance δ_{max} is defined [17] and an undirected graph is constructed from the generated microstructure. The edges (junction between cylinders) of the graph are assigned if the minimum separation distance (Δ) is less than δ_{max}. For each data point (set of material parameters) of the results shown in the next section, ten different microstructures were simulated and all the respective graph properties were averaged. The generated microstructure corresponds to a cube with side L_Ω equal to three times the length of the cylinder. Cubes filled with cylinders with aspect ratios of 100, 300 and 500 were simulated. The generated volume fractions ranged from 0.0001 to 0.01 for all aspect ratios. These microstructures corresponds to graphs where the number of vertices (N cylinders), is in the range $4 \times 10^2 \leq N \leq 4 \times 10^6$.

4.3 Results and discussion

The results for the critical volume fraction obtained experimentally [14] (0.002) are lower than those predicted by the excluded volume theory calculated using Eq. (4.1): $0.0067 \leq \Phi_c \leq 0.135$ for an aspect ratio of 100. This fact led us to consider that the percolation threshold for this type of nanocomposites must be also related to the matrix and not only dependent on the VGCNF network. To test that assumption, several microstructures were studied using a recently developed computer code[17, 18], created using the procedure described in the methods section. A maximum value for the minimum separation distance δ_{max} is defined [17] and an undirected graph is constructed from the generated microstructure. The δ_{max} parameter enables studying the influence of the matrix on the composite percolation threshold after the generation of the microstructure, as described latter. The analyses of some graph properties revealed that the microstructures can be described as random graphs. As shown in Fig. 4.1, percolation occurs at $\langle z \rangle = 1$ as predicted by [9],the giant component size (S) follows the relation: $S = 1 - \exp(-zS)$ as estimated by [10] and the degree distribution $P(z)$,Fig. 4.1 (inset), approaches a Poisson distribution as demonstrated by [9, 19]. Also, in Fig. 4.1 (inset), the $\langle z \rangle$ calculated from the Poisson distribution,$P(z) = \frac{e^{-\langle z \rangle} \langle z \rangle^z}{z!}$, to the data equals the ones obtained from direct calculation $(1.3, 1.9, 3.0)$. These results lead to the conclusion that the microstructure generated through a sequential pack algorithm [16] can be described by a random graph. Thus, the percolation problem

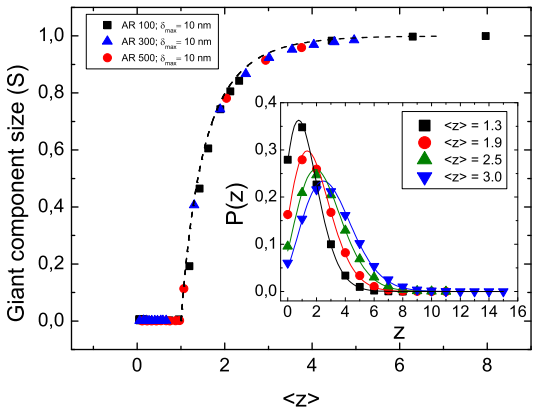

Figure 4.1: Simulation results for the composites with fiber aspect ratios of 100, 300 and 500 with $\delta_{max} = 10nm$. Main graph size of the giant component versus average degree, the line exhibits the relation[10]: $S = 1 - \exp(-zS)$ as expected for random graphs. Inset, plot of the degree distribution $P(z)$ for materials with different values of $\langle z \rangle$ with an aspect ratio of 300 and δ_{max} equal to $10nm$. The lines in the inset indicate the results of Poisson distribution fits to the data, with $R^2 \sim 0.99$ for all fits.

can be studied with these simple structures, knowing the fact that the phase transition in random graphs shares the same universality class with the mean field percolation [11]. It is important to mention that in the thermodynamic limit $N \to \infty$ the random graph approaches a Bethe lattice [10] confirming the experimental results of [14], i. e., $\beta \approx 1$. Furthermore, it should be considered that a nanocomposite microstructure can be anisotropic, leading to correlations between the degrees of neighboring vertices and hence to different values for the critical exponents, as discussed by Goltsev *et al* [20] in the context of complex networks models.

In Fig. 4.2, it can be observed, for different aspect ratios and δ_{max}, a linear relation between the average degree $\langle z \rangle$ and the volume fraction. Using the linear relations demonstrated in Fig. 4.2 between volume fraction and average degree and also the relation between edge number (m) and average degree: $\langle z \rangle = \frac{2m}{N}$, one obtains the following expression:

$$\Phi = \frac{D^2 \langle z \rangle}{2L\delta_{max}} \tag{4.5}$$

where D is the cylinder diameter and L the cylinder length. If in equation (4.5) we use $\langle z \rangle = 1$ in equation (4.5), the percolation threshold for a random graph be written as: $\Phi_c = \frac{D^2}{2L\delta_{max}}$. The latter equation holds when $\delta_{max} = D$, reproducing the results from the excluded volume theory [21, 22]. The previ-

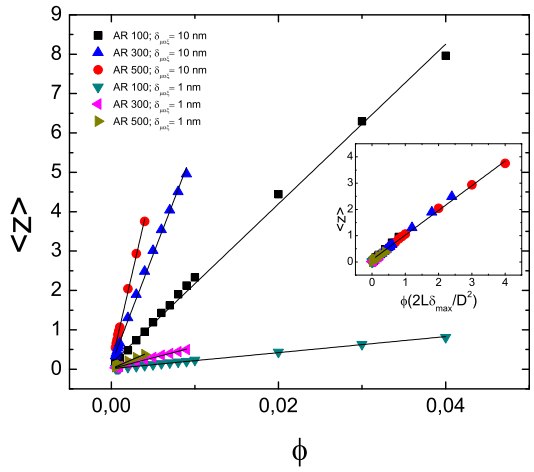

Figure 4.2: Dependence of the average degree on the volume fraction averaged over 10 different runs. $R^2 = 0.99$ for all fits. Inset: average degree versus scaled volume fraction, demonstrating the linear relation between the $\langle z \rangle$ and $\Phi \frac{2L\delta_{max}}{D^2}$.

ous equation, obtained within the framework of the complex network theory, can also be found in [23] with a different notation. The authors in [23] arrive to the same conclusion using a more complex approach based on the continuum connectedness percolation theory, while relying on some approximations. It is worthwhile to point out that the 1/2 factor, related to the average degree and edge number, is almost exact ($\pm 10^{-12}$) unlike some recent numerical simulations for hard rods (~ 0.6) [24, 25].

As the matrix for this type of composites is a dielectric and the typical size of the VGCNF is in the nanometer range, the assumption of hopping conductivity between the fillers mediated by the dielectric matrix seems plausible. The formula developed by Miller *et. al.* [26, 27] for the hopping conductivity can be stated as:

$$\sigma_{ij} = \sigma_0 \exp\left(-\frac{x_{ij}}{x_0} - \frac{\epsilon_{ij}}{k_B T}\right) \tag{4.6}$$

where x_{ij} is the distance between two fillers, in this work the minimum distance between two VGCNF, x_0 is the scale over which the wave function decays in the matrix, $\frac{\epsilon_{ij}}{k_B T}$ is the thermal hopping term, that can be neglected at room temperature, and σ_0 is the dimension coefficient. Bearing in mind Eq. (4.6) for the conductivity between two fillers, a similarity with recent results for the conductance distribution [28] obtained on Erdös and Rény random graphs and also for the current flow on random resistor networks [29] is observed.

In these studies, the general expression that relates an edge weight to the conductance is stated as:

$$G_{ij} = \exp\left(-a x_{ij}\right) \tag{4.7}$$

Eq. (4.7) links two arbitrary vertices with an edge weight that corresponds to the conductance between two vertices. It should be noted here that the distinction between conductance and conductivity is just a geometrical factor and a direct proportionality exists between the two physical quantities. Eq. (4.7) is similar to Eq. (4.6) at room temperature. In Eq. (4.7), the constant a controls the disorder strength or the dimensionless mean hopping and $x_{ij} \in [0, 1]$ is taken from a uniform distribution. Our distributions for the minimum separation distance (Δ) are uniform, defining $\Delta = D + \delta_{max}\,[0, 1]$,where D is the cylinder diameter. By rearranging the expression, dividing by some characteristic length (ξ), $\frac{\Delta - D}{\xi} = \frac{\delta_{max}}{\xi}$ and setting the disorder constant a to: $a = \frac{\delta_{max}}{\xi}$, the results of [28, 29] can be applied in order to find a general expression for the VGCNF/polymer composites conductance. The physical origins of the defined disorder constant will be discussed later in this chapter.

From [29] it was obtained that $\frac{R}{R_{cut}} \sim \exp\left(\frac{a}{L^{\frac{1}{v}}}\right)$, where v is the percolation connectivity exponent (which is an universal exponent, independent of filler geometry or spatial arrangement), R the resistance and R_{cut} the cut resistance. R_{cut} can be understood as the equivalent resistance of the system after cutting the bond with the maximal local current. After cutting, the current will reorganize to follow a new optimal path. Wu *et. al.* [29] also found that the ratio L/a^{ν} characterizes the disorder and determines the properties of current flow. Setting $v = \frac{1}{2}$ for a random graph when $N \to \infty$ and using the relation $L \sim N^{\frac{1}{d_c}}$, where L is the lattice linear size and $d_c = 6$ is the critical dimension of percolation for random graphs, an equation for the conductance is obtained:

$$G_{eff} = G_{cut} \exp\left(\frac{-a}{(b\Phi)^{\frac{1}{3}}}\right) \tag{4.8}$$

where b is equal to the volume of the domain divided by the volume of the filler,i.e., $b = \frac{V_{\Omega}}{V_{filler}}$ and G_{cut} is the effective conductance of the system before a bond with maximum conductance is added to (or removed from) the system [12]. The disorder, a, in Eq. (4.8) is the parameter that controls the broadness of the distribution of linked weights [12].

In Fig. 4.3 the results of the electrical conductivity as a function of the volume fraction for two types of VGCNF, pristine and functionalized ones, are shown. Interestingly, it is observed that the two composites follows a $\log(\sigma) \propto \Phi^{-\frac{1}{3}}$ relationship, independently of the functionalization of the fillers.

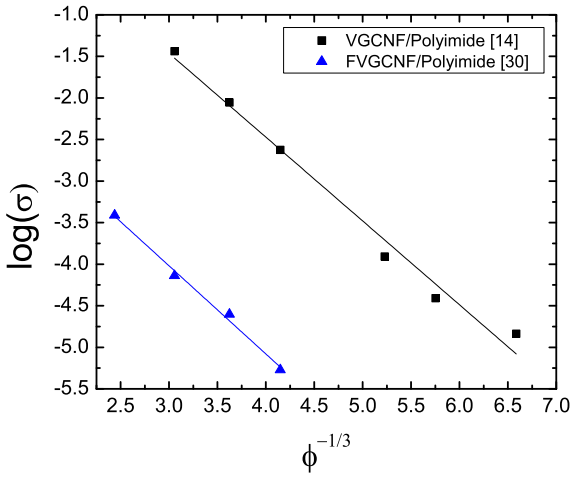

Figure 4.3: Logarithm plot of the conductivity for two types of fillers, vapour grown carbon nanofibers (VGCNF), functionalized[30] (FVGCNF) and pristine[14] (VGCNF), versus volume fraction.

Though the physical mechanism is different there is a formal similarity between Eq. (4.8) ($\Phi^{-\frac{1}{3}}$ dependence) and the expression for fluctuation-induced tunneling[31]:

$$\sigma_{DC} \propto \exp(-2\chi_T d) \tag{4.9}$$

where $\chi_T = \sqrt{\frac{2mV(T)}{h^2}}$, m represents the mass of the charge carriers, d the barrier width and V(T) the temperature modified barrier height. Usually, it must be assumed a random distribution of particles to make use of the following proportionality[32] $d \sim \Phi^{-\frac{1}{3}}$. As can be seen in recent works[33, 8] and in Fig. 4.3, if the conductivity of the composite can be described by Eq. (4.9), then it leads to the following dependence:

$$\log(\sigma_{DC}) \sim \Phi^{-\frac{1}{3}} \tag{4.10}$$

Applying the logarithm to both sides of Eq. (4.8) and using the previous relation for the conductance leads to $\frac{a}{b^{\frac{1}{3}}} = 1$. Then:

$$a = b^{\frac{1}{3}} \tag{4.11}$$

where V_Ω is the volume of the domain and V_{filler} is the volume of the filler. The right hand side of Eq. (4.11),b, is simply the total number of fillers that can exist in the domain N_{max}. It is known[13] that the length of the optimal path in the strong disorder regime, ℓ_{opt}, can be related to the system

size by: $\ell_{opt} \sim N_{max}^{\frac{1}{3}}$. Replacing N_{max} and ℓ_{opt} in Eq. (4.11): $a = \ell_{opt}$. The latter equality states that the disorder constant is equal to the length of the optimal path in the strong disorder regime. This indicates that Eq. (4.10) corresponds to the weak disorder case. This can be supported by following the methodology developed by Sreenivasan *et. al.* [12]. One starts with two random numbers r_1 and r_2, such that $r_1 > r_2$, in the present case defined as the minimum distance between two cylinders and they differ by one order of magnitude. With $\Delta r = r_1 - r_2$, the following expression is obtained:

$$\frac{G_1}{G_2} = \exp\left(-a\Delta r\right) \tag{4.12}$$

The case when $-a\Delta r \ll -1$ corresponds to the strong disorder case, and the limit $-a\Delta r \sim -1$ corresponds to the weak disorder limit, where all weights becomes of the same order of magnitude. For a uniform distribution of the edges weights[12] $\Delta r \sim \frac{1}{\ell_{opt}}$ for a optimal path in the strong disorder limit with length ℓ_{opt}. Making the substitution in the expression for the weak disorder case, $a\frac{1}{\ell_{opt}} \sim 1$, then:

$$a = \frac{\delta_{max}}{\xi} \sim \ell_{opt} \tag{4.13}$$

It was already arrived to Eq. (4.13) previously, by a different route. It can be then stated that the conductance described by Eq. (4.8), when Eq. (4.10) is obeyed, corresponds to the weak disorder case. One important question that arises is the possibility of the existence of a strong disorder regime in our system. In [34] Chen *et. al.* studied the statistics of optimal paths in random and scale-free networks demonstrating,for several weight distributions, that a strong disorder regime and a transition to weak disorder is observed. They also found a single parameter, s, that determines the disorder strength and the disorder crossover. For $s \ll 1$ the system is in the weak disorder limit and for $s \to 1$ the system is in the strong disorder limit. Chen *et. al.*[34] showed that for an exponential "disorder function" $f(x) = e^{ax}$ where x is a random number between 0 and 1 and a the disorder strength constant, this function is similar to Eq. (4.7), a crossover from strong to weak disorder is observed. For $f(x) = e^{ax}$ they determined that $s = ap_cN^{-\frac{1}{3}}$. In our case $p_c = 1/ < k >$ for a random graph [9] leading to $s \ll 1$,i.e., the weak disorder case. So our system is always in the weak disorder regime. Another important fact is that the correlation length ξ is just $\frac{\delta_{max}}{\ell_{opt}}$ or a division between a parameter δ_{max} that is determined by the matrix and the length of the optimal path in the strong disorder case. Substituting Eq. (4.13) in Eq. (4.8):

$$G_{eff} = G_{cut} \exp\left(\frac{-\ell_{opt}}{(N_{max}\Phi)^{\frac{1}{3}}}\right) \tag{4.14}$$

As final considerations for Eq. (4.14) two cases must be considered: a) $N_{max}^{\frac{1}{3}} \sim \ell_{opt}$: implying that $G_{eff} = G_{cut} \exp\left(-\frac{1}{\Phi^{\frac{1}{3}}}\right)$, i. e., the weak disorder case as previously discussed; b) $\Phi < \Phi_c$: implies that $G_{eff} \sim G_{cut}$ due to the fact that $\langle z \rangle \ll 1$. From the latter it is clear that the best effective conductance is achieved trough a compromise between the number of fibers and the the length of the optimal path. It also seems that a good distribution of clusters,as represented in Fig. 4.4 for four clusters, will reduce the N_{max} and hence the length of the optimal path. This is due to the fact that each cluster of connected fibers is mapped to a single vertice in the network, instead of having one vertice for each fiber. This results in a lower number of vertices. As a final remark to

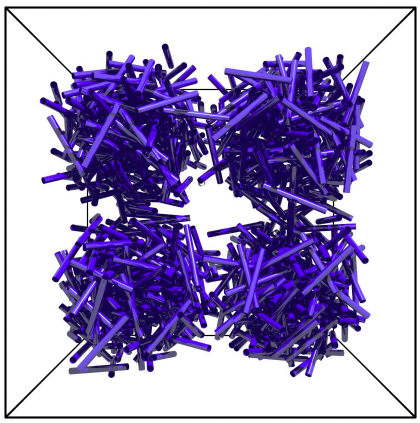

Figure 4.4: Representation of a possible material with four clusters evenly distributed in the domain.

the applicability of Eq. (4.14), from the latter statements, G_{cut} will depend on the matrix properties, as demonstrated in [35, 36].

4.4 Conclusion

Here we show that the microstructure generated by a derivation of sequential packing algorithm can be described by a random graph, where the vertices correspond to rods and the edges to the junction between them. This approach

is not limited to rod-like fillers and can be easily extended to other fillers with different geometry. It is shown that the conduction in VGCNF/polymer composites can be described by a Bethe lattice confirming recent experimental results. Through the use of the complex network framework, an expression is obtained for the percolation threshold. In the same way, it is demonstrated that hopping between adjacent fillers gives rise to an expression, $\log(\sigma_{DC}) \sim \Phi^{-\frac{1}{3}}$, that corresponds to a weak disorder regime.

4.5 References

[1] J. Silva, R. Simoes, S. Lanceros-Mendez, R. Vaia, Applying complex network theory to the understanding of high aspect ratio carbon filled composites, Europhysics Letters (EPL) 93 (2011) 37005.

[2] E. T. Thostenson, C. Li, T.-W. Chou, Nanocomposites in context, Composites Science and Technology 65 (2005) 491.

[3] D. Stauffer, A. Aharony, Introduction to Percolation Theory, Taylor and Francis, London, 1992.

[4] A. Celzard, E. McRae, C. Deleuze, M. Dufort, G. Furdin, J. F. Marêché, Critical concentration in percolating systems containing a high-aspect-ratio filler, Physical Review B 53 (1996) 6209.

[5] S. H. Munson-McGee, Estimation of the critical concentration in an anisotropic percolation network, Physical Review B 43 (1991) 3331.

[6] L. Berhan, A. M. Sastry, Modeling percolation in high-aspect-ratio fiber systems. II. The effect of waviness on the percolation onset, Physical Review E 75 (2007) 41121.

[7] L. Berhan, A. M. Sastry, Modeling percolation in high-aspect-ratio fiber systems. I. Soft-core versus hard-core models, Physical Review E 75 (2007) 41120.

[8] W. Bauhofer, J. Z. Kovacs, A review and analysis of electrical percolation in carbon nanotube polymer composites, Composites Science and Technology 69 (2009) 1486.

[9] P. Erdös, A. Rény, On random graphs, Publicationes Mathematicae 6 (1959) 290.

[10] M. E. J. Newman, The Structure and Function of Complex Networks, SIAM Review 45 (2003) 167.

[11] R. Albert, A.-L. Barabási, Statistical mechanics of complex networks, Reviews of Modern Physics 74 (2002) 47.

[12] S. Sreenivasan, T. Kalisky, L. A. Braunstein, S. V. Buldyrev, S. Havlin, H. E. Stanley, Effect of disorder strength on optimal paths in complex networks, Physical Review E 70 (2004) 046133.

[13] L. Braunstein, S. Buldyrev, R. Cohen, S. Havlin, H. Stanley, Optimal Paths in Disordered Complex Networks, Physical Review Letters 91 (2003) 168701.

[14] A. Trionfi, D. H. Wang, J. D. Jacobs, L. S. Tan, R. A. Vaia, J. W. P. Hsu, Direct Measurement of the Percolation Probability in Carbon Nanofiber-Polyimide Nanocomposites, Physical Review Letters 102 (2009) 116601.

[15] R. Simoes, J. Silva, R. Vaia, A Complex Network Based Simulation Approach to Predict the Electrical Properties of Nanocomposites, Journal of Nanoscience and Nanotechnology 10 (2010) 2451.

[16] M. J. Vold, Sediment Volume and Structure in Dispersions of Anisometric Particles, The Journal of Physical Chemistry 63 (1959) 1608.

[17] R. Simoes, J. Silva, R. Vaia, V. Sencadas, P. Costa, J. Gomes, S. Lanceros-Mendez, Low percolation transitions in carbon nanotube networks dispersed in a polymer matrix: dielectric properties, simulations and experiments, Nanotechnology 20 (2009) 35703.

[18] R. Simoes, J. Silva, A. Cadilhe, R. Vaia, Applications of the Graph Theory to the Prediction of Electrical and Dielectric Properties of Nano-filled Polymers, Composite Interfaces 17 (2010) 407.

[19] B. Bollobás, Degree sequences of random graphs, Discrete Mathematics 33 (1981) 1.

[20] A. V. Goltsev, S. N. Dorogovtsev, J. F. F. Mendes, Percolation on correlated networks, Physical Review E 78 (2008) 051105.

[21] I. Balberg, C. H. Anderson, S. Alexander, N. Wagner, Excluded volume and its relation to the onset of percolation, Physical Review B 30 (1984) 3933.

[22] A. L. R. Bug, S. A. Safran, I. Webman, Continuum Percolation of Rods, Physical Review Letters 54 (1985) 1412.

[23] A. V. Kyrylyuk, P. van der Schoot, Continuum percolation of carbon nanotubes in polymeric and colloidal media, Proceedings of the National Academy of Sciences 105 (2008) 8221.

[24] Z. Néda, R. Florian, Y. Brechet, Reconsideration of continuum percolation of isotropically oriented sticks in three dimensions, Physical Review E 59 (1999) 3717.

[25] M. Foygel, R. D. Morris, D. Anez, S. French, V. L. Sobolev, Theoretical and computational studies of carbon nanotube composites and suspensions: Electrical and thermal conductivity, Physical Review B 71 (2005) 104201.

[26] V. Ambegaokar, Theory of hopping conductivity in disordered systems, Journal of Non-Crystalline Solids 8-10 (1972) 492.

[27] A. Miller, E. Abrahams, Impurity Conduction at Low Concentrations, Physical Review 120 (1960) 745.

[28] G. Li, L. A. Braunstein, S. V. Buldyrev, S. Havlin, H. E. Stanley, Transport and percolation theory in weighted networks, Physical Review E 75 (2007) 45103.

[29] Z. Wu, E. López, S. V. Buldyrev, L. A. Braunstein, S. Havlin, H. E. Stanley, Current flow in random resistor networks: The role of percolation in weak and strong disorder, Physical Review E 71 (2005) 45101.

[30] M. J. Arlen, D. Wang, J. D. Jacobs, R. Justice, A. Trionfi, J. W. P. Hsu, D. Schaffer, L.-S. Tan, R. A. Vaia, Thermal-Electrical Character of in Situ Synthesized Polyimide-Grafted Carbon Nanofiber Composites, Macromolecules 41 (2008) 8053.

[31] M. T. Connor, S. Roy, T. A. Ezquerra, F. J. Baltá Calleja, Broadband ac conductivity of conductor-polymer composites, Physical Review B 57 (1998) 2286.

[32] H. Kawamoto, E. J. Sichel, Carbon black-polymer composites, Marcel Dekker, New York, 1982.

[33] P. Cardoso, J. Silva, A. J. Paleo, F. W. J. van Hattum, R. Simões, S. Lanceros-Mendez, The dominant role of tunneling in the conductivity of carbon nanofiber-epoxy composites, Physica Status Solidi A 207 (2009) 407.

[34] Y. Chen, E. Lopez, S. Havlin, H. E. Stanley, Universal Behavior of Optimal Paths in Weighted Networks with General Disorder, Physical Review Letters 96 (2006) 68702.

[35] P. Costa, J. Silva, V. Sencadas, C. M. Costa, F. W. J. van Hattum, J. G. Rocha, S. Lanceros-Mendez, The effect of fibre concentration on the [alpha] to [beta]-phase transformation, degree of crystallinity and electrical properties of vapour grown carbon nanofibre/poly(vinylidene fluoride) composites, Carbon 47 (2009) 2590–2599.

[36] X. Sun, M. Song, Highly Conductive Carbon Nanotube/Polymer Nanocomposites Achievable?, Macromolecular Theory and Simulations 18 (2009) 155.

5

Critical behavior of a three-dimensional hardcore-cylinder composite system

In this chapter the critical indices β, γ and ν for a three-dimensional hardcore cylinder composite system with short-range interactions have been obtained. In contrast to the 2D stick system and the 3D hard-core cylinder system, the determined critical exponents do not belong to the same universality class as the lattice percolation, although obeying to the common hyperscaling relation for a 3D system. It is observed that the value of the correlation length exponent is compatible with the predictions of the mean field theory. It is also shown that, by using the Alexander-Orbach conjuncture, the relation between the conductivity and the correlation length critical exponents has a typical value for a 3D lattice system. This chapter is based on [1].

5.1 Introduction

The percolation problem of 2D random sticks was first addressed by Pike *et. al* [2], with the authors focusing on the determination of the point of emergence of the giant component that spans the system, i. e., the percolation threshold [3, 4]. Later, Balberg *et. al* [5] derived the percolation critical exponents for the 2D random sticks problem, demonstrating that the 2D continuum percolation problem belongs to the same universality class as the lattice percolation, i.e., the continuum and the lattice percolation problems share the same critical exponents. The latter is in agreement with the expected universality of the critical exponents, as they depend just on the system dimension, the symmetry of the order parameter and on the range of interactions [6]. It was also established that the percolation threshold is proportional to the inverse of the expected excluded volume (3D) or area (2D) of the stick, i. e., the volume (area) around a object into which the center of another similar object is not allowed to enter [7, 8, 9]. With carbon nanotubes [10] and their wide application range [11], the percolation problem of 2D and 3D random rods becomes an essential framework to study the experimental results of the growing field of

carbon nanotube/polymer composites. One of the first works comparing experimental results on polymers reinforced with carbon fibers with the theoretical predictions from the exclude volume theory and determining the bounds for the percolation threshold of high aspect ratio rods, was presented by Clelzard *et. al* [12]. This work was followed by studies related to the determination of the percolation threshold of 2D or 3D rods systems [13, 14, 15, 16, 17, 18, 19, 20]. The relevance of these works for the material science field was recently summarized in a review article [21]. Remarkably, while for the 2D soft-core problem the determination of the critical exponents has been reported [5], few studies [22, 23, 24] are focused on the determination of the critical exponents for 3D hard-core caped cylinders with an isotropic distribution. In fact, in the works of Dani *et. al* [23, 24] and Ogale *et. al* [22] the system has some degree of anisotropy in order to better model the composite processing conditions and the hard-core fillers have a low aspect ratio. In this way, Dani *et. al* [23, 24] calculated the γ, σ, τ and ν critical exponents and the fractal dimension of the 3D continuum short-fiber composite. It was found that the values of the critical exponents are in agreement with the values for the 2D and 3D lattice systems and 2D continuum systems reported in the literature. The correlation length critical exponent was also calculated [22] and it was found that it is in agreement with the values for 3D lattice systems. A recent experimental study for carbon nanofiber/polyimide composites [25] determined the critical geometrical exponent, β, reporting that it belongs to the same universality class of a Bethe lattice, i.e, $\beta = 1$. This experimental result has been theoretically explained [26] through the application of the network theory to carbon nanofiber nanocomposites, by mapping fillers to vertices and edges to the gap between fillers.

In this chapter, the critical behaviour for composites filled with high-aspect ratio cylinders interacting with each other by a short-range potential is analysed. The critical exponents β, γ and ν are calculated using a finite size scaling analysis [3] with the objective of clarifying previous studies on the dimension of the clusters criticality for an isotropic systems with hard-core fillers with an high aspect ratio.

5.2 Methods

The microstructure for the isotropic materials is generated by a derivation of a sequential packing algorithm [27] to place randomly oriented cylinders in 3D space and using periodic boundary conditions, i. e, when part of a cylinder crosses the domain boundary it is cut and the segment that crosses the boundary is translated to the opposite domain boundary (i. e, symmetrically

translated). After creating the virtual composite, the graph theory framework was used to study the composites percolation threshold. Within this framework, the cylinders are mapped to vertices and the edges to the minimum distance between the cylinders, which corresponds to the maximum electric field between the two fillers [28]. A maximum value for the minimum separation distance δ_{max} is defined [28] and an undirected graph is constructed from the generated microstructure. The edges (junction between cylinders) of the graph are assigned if the minimum separation distance is less than δ_{max}. The generated microstructure corresponds to a cube with side L and five different cube side lengths were simulated, $L = 300, 400, 500, 600, 700$. Cubes were filled with cylinders with aspect ratios of 100 and $\delta_{max} = 1$ and the generated volume fractions ranged from 10^{-4} to 4.1×10^{-3}, corresponding to a number of cylinders from a few hundred to $\sim 10^4$. It is stressed that by increasing the δ_{max} value the number of connected cylinders is increased shifting the percolation threshold to lower values.

For each data point (set of material parameters) of the results shown, $\sim 10^4$ different microstructures were simulated and all the respective graph properties were averaged. More precisely, using a breadth-first search algorithm [29] the size of the largest component, giant component S, was calculated by monitoring the size distribution, $P(s)$, of finite clusters, excluding the size of the largest cluster, to which a randomly node belongs, $P(s) = sn(s)/s_{av}$. Here, s is the number of vertices, $n(s)$ is the cluster size distribution and s_{av} is the ratio of the number of vertices to the total number of clusters. By knowing $P(s)$, the size of the giant component can be calculated, $S = 1 - \sum_s P(s)$ as well as the mean size of a finite cluster to which a random vertex belongs, $\langle s \rangle = \sum_s sP(s)$.

5.3 Results and Discussion

In Fig. 5.1 (a) is presented the evolution of the size of the giant component, S, as a function of the volume fraction for different domains sizes. In the same Fig. 5.1 (b) is shown the mean size of the finite clusters, $\langle s \rangle$, as a function of the cylinder volume fraction. Also in Fig. 5.1 (b) it is observed that the maximum value of $\langle s \rangle$ increases with increasing system size and it is possible to extrapolate that when $L \to \infty, \langle s \rangle \to \infty$ at the percolation threshold. In the system under study the size of the giant component, S, takes the role of the order parameter and the mean size of the finite clusters,$\langle s \rangle$, takes the role of the susceptibility [30]. It is observed in Fig. 5.1 that the order parameter changes continuously and the susceptibility diverges at the percolation threshold. The order parameter takes the value of zero in the most symmetric phase and non-zero in the least symmetric phase , e.g. there is a symmetry break or

change at the phase transition. If the order parameter changes continuously at the percolation threshold and there is a divergence in the susceptibility the transition is termed second-order Fig. 5.1.

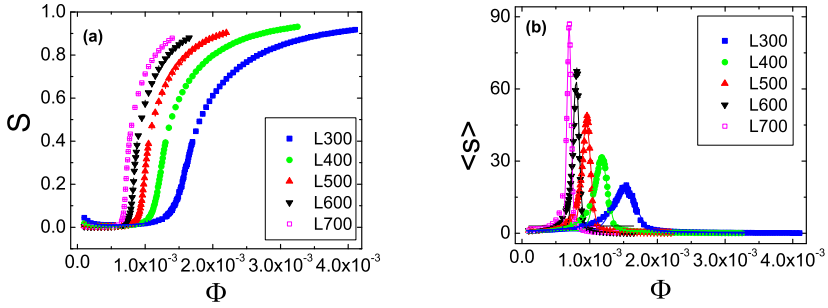

Figure 5.1: (a): Size of the giant component as a function of the volume fraction. (b): Size of the finite cluster, excluding the giant component, as a function of the volume fraction. Results have been averaged over $\sim 10^4$ samples. Error bars are smaller than the data points.

It is known [3] that for a second order phase transition the width of the transition, Δ, should scale with system size as $\Delta \sim L^{-\frac{1}{\nu}}$ where ν is related with correlation length, ξ. The width of the transition can be naturally calculated by fitting $\langle s \rangle$ to a Gaussian and using the full width at half maximum (FWHM), of the Gaussian as the value for Δ. Another approximation [3] is using a Gaussian to fit $\frac{dS}{d\phi}$ as a function of ϕ and taking the value of the Gaussian FWHM as the value for Δ. The two methods, previously described, were employed in the determination of Δ and the results are summarized in Fig. 5.2. In Fig. 5.2, one can observe that in a log-log scale there is a linear relationship between the width of the transition, Δ, and the length of the domain, L.

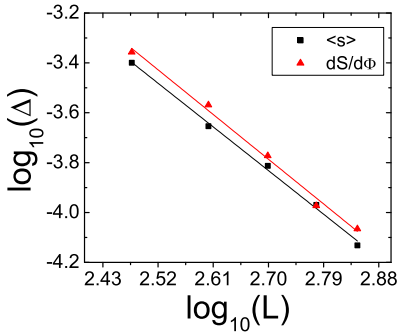

Figure 5.2: Width of the transition versus system dimension in a log-log plot.The lines are linear fits to the data

As can be observed in Fig. 5.2 the two methods give similar results. More precisely, the calculated correlation length critical exponents are $\nu = 0.502 \pm 0.022$ for the method based on the order parameter and $\nu = 0.514 \pm 0.016$ for the method based on the susceptibility. The latter values lead to the conclusion that ν is compatible with the mean field value, i. e., $\nu = 1/2$. Once the value for the correlation length exponent is obtained, it is possible to determine other critical exponents using a finite size scaling analysis (FSS) [3]. It should be pointed that FSS analyses have already been successfully applied to networks [31]. In this chapter it is used the volume fraction, ϕ, as control parameter instead of the number of vertices due to the fact that the former can be easily related to experimental works. As the two parameters are related by a linear relation it is expect that the obtained critical exponents will be the same. Close to the critical volume fraction, the correlation length, ξ, is comparable to the system size and therefore the size of the giant cluster, S should scale as:

$$S = L^{-\frac{\beta}{\nu}} F\left[L^{\frac{1}{\nu}}(\phi - \phi_c)\right] \tag{5.1}$$

where F is a suitable scaling function. The FSS also predicts that $\langle s \rangle$ should scale with the system size L as:

$$\langle s \rangle = L^{\frac{\gamma}{\nu}} F_1\left[L^{\frac{1}{\nu}}(\phi - \phi_c)\right] \tag{5.2}$$

where the scaling function, F_1, in Eq.(5.2) is different from the one in Eq.(5.1). The latter equations are expected to scale at $\phi = \phi_c$ as power laws. Using the ϕ_c and the height of the Gaussian fits to $\langle s \rangle$, presented in Fig. 5.1 (b), it is possible to use the latter scaling relations to obtain the critical exponents. For the determination of $\frac{\beta}{\nu}$, the size of the giant component at ϕ_c for the different domain sizes was used, as presented in Fig. 5.3 (a) in a double logarithm scale.

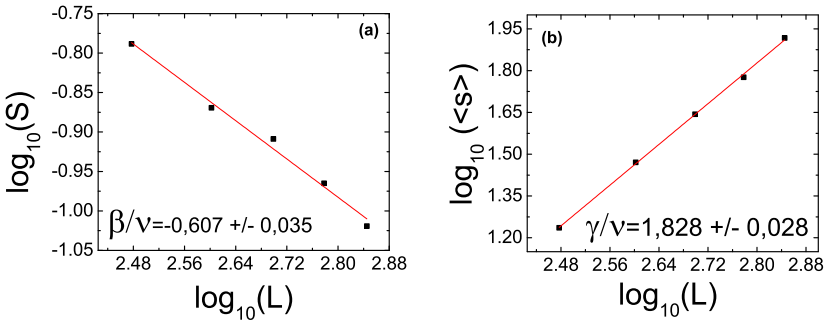

Figure 5.3: (a): Double logarithm plot of the size of the giant component, at ϕ_c, for the different domain sizes, L. (b): Double logarithm plot of the height of the fitted Gaussian for the different domain sizes, L

To establish the value of $\frac{\gamma}{\nu}$, the height of the fitted Gaussian for the different domains sizes were plotted in a double logarithm scale as shown in Fig. 5.3 (b). The linear relations that are obtained in Fig. 5.3, $R^2 \sim 0.99$ for the two fits, demonstrate that the two scaling laws, Eq.(5.1) and Eq.(5.2), are obeyed.

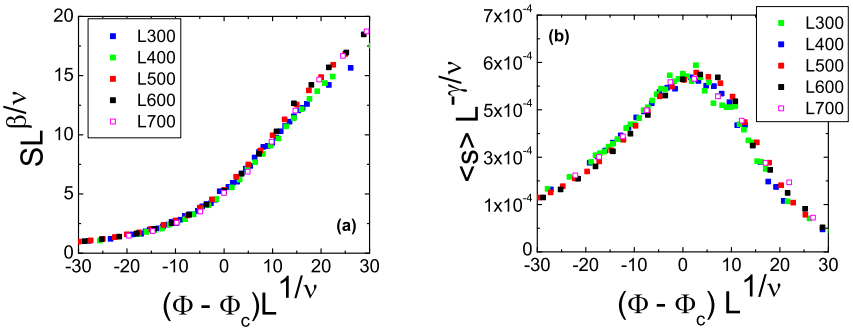

Figure 5.4: (a): $SL^{\frac{\beta}{\nu}}$ vs $(\Phi - \Phi_c)L^{\frac{1}{\nu}}$. (b):$\langle s \rangle L^{-\frac{\gamma}{\nu}}$ vs $(\Phi - \Phi_c)L^{\frac{1}{\nu}}$

The FSS theory also predicts that near ϕ_c the curves for the different domain sizes should collapse in one curve. It is possible to observe this fact in Fig. 5.4 (a) for the order parameter and in Fig. 5.4 (b) for the susceptibility. Using the obtained values for ν it is possible to determine β and γ. So, $\beta = 0.305 \pm 0.022$ using $\nu = 0.502 \pm 0.022$ and $\beta = 0.312 \pm 0.020$ using $\nu = 0.514 \pm 0.016$. The obtained values for γ are: $\gamma = 0.918 \pm 0.043$ using $\nu = 0.502 \pm 0.022$ and $\gamma = 0.940 \pm 0.033$ using $\nu = 0.514 \pm 0.016$ which are close to the mean field value, $\gamma = 1.0$. Interestingly, it is known that the hyperscaling relation [3, 4]:

$$d = 2\frac{\beta}{\nu} + \frac{\gamma}{\nu} \tag{5.3}$$

should be obeyed up to the critical dimension, $d_c \leq 6$. Using Eq.(5.3) with the critical exponents calculated from the data presented in Fig. 5.3, then $d = 3.041 \pm 0.075$ which is in accordance with the 3D system. The reported critical exponents do not agree with the critical exponents for the 3D lattice universality class [3, 4], i. e, $\beta_{3D} = 0.4$, $\gamma_{3D} = 1.8$ and $\nu_{3D} = 0.9$. As the latter exponents are not exact values we round them to the first decimal place. On the other hand, our calculated values for β and ν have been found in experimental work [32] related to the critical behaviour of a phase transition in the near surface region. Interestingly, another model that exhibits a tricritical point and shares the same critical exponent, $\beta = 0.3$, was recently proposed by Cellai *et. al* [33] in the context of the k-core percolation. The values of the obtained critical exponents can be used to calculate the conductivity critical exponent which is known to follow a power law: $\sigma \sim (\phi - \phi_c)^t$, where σ is the

system conductivity. For a 3D system and using the previous critical exponents [3]:

$$\frac{t}{\nu} \sim 2.2 \tag{5.4}$$

The obtained value of Eq.(5.4) can be also deduced by the determined critical exponents using the Alexander-Orbach conjuncture [34]. The Alexander-Orbach conjuncture is based on the diffusion on fractals and predicts that the dimensionality of the quantized vibrational states on a fractal is close to $\frac{4}{3}$ for $d \geq 2$, independent of the system dimensionality. The latter implies that:

$$\frac{t}{\nu} = \frac{1}{2}(3d-4) - \frac{\beta}{2\nu} \tag{5.5}$$

Solving Eq.(5.5) for a 3D system and with the calculated $\frac{\beta}{\nu}$ from Fig. 5.3, results in $\frac{t}{\nu} = 2.197 \pm 0.018$ which is in accordance to Eq.(5.4), within the determined error, for a 3D system. In particular the t has a value of 1.103 ± 0.049 using $\nu = 0.502 \pm 0.022$ and 1.129 ± 0.036 using $\nu = 0.514 \pm 0.016$. The latter values are close to the one, 1.0, obtained by the effective medium theory [35].

5.4 Conclusion

In conclusion, the critical exponents for a hard-core 3D cylinder system with short-range interactions has been obtained, making use of the network theory, and these are related through the common hyperscaling for a 3D system. In contrast to the 2D stick system and the 3D hard-core cylinder system, the determined critical exponents do not belong to the same universality class as the lattice percolation. Instead, the correlation length critical exponent has a typical mean field value, the γ critical exponent has a value that is close to the mean field one, and $\beta = 0.3$. Interestingly, using the Alexander-Orbach conjuncture, it is found that the relation between the conductivity and the correlation length critical exponents for a 3D system is obeyed.

5.5 References

[1] J. Silva, R. Simoes, S. Lanceros-Mendez, Critical behavior of a three-dimensional hardcore-cylinder composite system, Physical Review E 85 (2012) 021115.

[2] G. E. Pike, C. H. Seager, Percolation and conductivity: A computer study. I, Physical Review B 10 (1974) 1421.

[3] D. Stauffer, A. Aharony, Introduction to Percolation Theory, Taylor and Francis, London, 1992.

[4] J. W. Essam, Percolation theory, Reports on Progress in Physics 43 (1980) 53.

[5] I. Balberg, N. Binenbaum, C. H. Anderson, Critical Behaviour of the two-dimensional sticks system, Physical Review Letters 51 (1983) 1605.

[6] R. B. Griffiths, Dependence of critical indices on a parameter, Physical Review Letters 24 (1970) 1479.

[7] I. Balberg, C. H. Anderson, S. Alexander, N. Wagner, Excluded volume and its relation to the onset of percolation, Physical Review B 30 (1984) 3933.

[8] I. Balberg, N. Binenbaum, Percolation Thresholds in the Three-Dimensional Sticks System, Physical Review Letters 52 (1984) 1465.

[9] A. L. R. Bug, S. A. Safran, I. Webman, Continuum Percolation of Rods, Physical Review Letters 54 (1985) 1412.

[10] S. Iijima, Helical microtubles of graphitic carbon, Nature 354 (1991) 56.

[11] R. H. Baughman, A. A. Zakhidov, W. A. de Heer, Carbon nanotubes–the route toward applications., Science 297 (2002) 787.

[12] A. Celzard, E. McRae, C. Deleuze, M. Dufort, G. Furdin, J. F. Marêché, Critical concentration in percolating systems containing a high-aspect-ratio filler, Physical Review B 53 (1996) 6209.

[13] S. H. Munson-McGee, Estimation of the critical concentration in an anisotropic percolation network, Physical Review B 43 (1991) 3331.

[14] M. Foygel, R. D. Morris, D. Anez, S. French, V. L. Sobolev, Theoretical and computational studies of carbon nanotube composites and suspensions: Electrical and thermal conductivity, Physical Review B 71 (2005) 104201.

[15] L. Berhan, A. M. Sastry, Modeling percolation in high-aspect-ratio fiber systems. II. The effect of waviness on the percolation onset, Physical Review E 75 (2007) 41121.

[16] L. Berhan, A. M. Sastry, Modeling percolation in high-aspect-ratio fiber systems. I. Soft-core versus hard-core models, Physical Review E 75 (2007) 41120.

[17] A. V. Kyrylyuk, P. van der Schoot, Continuum percolation of carbon nanotubes in polymeric and colloidal media, Proceedings of the National Academy of Sciences 105 (2008) 8221.

[18] A. P. Chatterjee, Percolation thresholds for rod-like particles: polydispersity effects, Journal of Physics:Condensed Matter 20 (2008) 255250.

[19] R. H. J. Otten, P. van der Schoot, Continuum Percolation of Polydisperse Nanofillers, Physical Review Letters 103 (2009) 225704.

[20] A. P. Chatterjee, Connectedness percolation in polydisperse rod systems: A modified Bethe lattice approach., Journal of Chemical Physics 132 (2010) 224905.

[21] C.-W. Nan, Y. Shen, J. Ma, Physical Properties of Composites Near Percolation, Annual Review of Materials Research 40 (2010) 131.

[22] A. A. Ogale, S. F. Wang, Simulation of the percolation behavior of quasi- and transversely isotropic short-fiber composites with a continuum model, Composites Science and Technology 46 (1993) 379.

[23] A. Dani, A. A. Ogale, Electrical percolation behavior of short-fiber composites: Experimental characterization and modeling, Composites Science and Technology 56 (1996) 911.

[24] A. Dani, A. A. Ogale, Percolation in short-fiber composites: Cluster statistics and critical exponents, Composites Science and Technology 57 (1997) 1355.

[25] A. Trionfi, D. H. Wang, J. D. Jacobs, L. S. Tan, R. A. Vaia, J. W. P. Hsu, Direct Measurement of the Percolation Probability in Carbon Nanofiber-Polyimide Nanocomposites, Physical Review Letters 102 (2009) 116601.

[26] J. Silva, R. Simoes, S. Lanceros-Mendez, R. Vaia, Applying complex network theory to the understanding of high aspect ratio carbon filled composites, Europhysics Letters (EPL) 93 (2011) 37005.

[27] M. J. Vold, Sediment Volume and Structure in Dispersions of Anisometric Particles, The Journal of Physical Chemistry 63 (1959) 1608.

[28] R. Simoes, J. Silva, R. Vaia, V. Sencadas, P. Costa, J. Gomes, S. Lanceros-Mendez, Low percolation transitions in carbon nanotube networks dispersed in a polymer matrix: dielectric properties, simulations and experiments, Nanotechnology 20 (2009) 35703.

[29] T. H. Cormen, C. E. Leiserson, R. L. Rivest, C. Stein, Introduction to algorithms, MIT Press, Cambridge, 2001.

[30] M. E. J. Newman, The Structure and Function of Complex Networks, SIAM Review 45 (2003) 167.

[31] H. Hong, M. Ha, H. Park, Finite-Size Scaling in Complex Networks, Physical Review Letters 98 (2007) 258701.

[32] B. Burandt, W. Press, S. Haussuhl, Near-Surface X-Ray Critical Scattering from a NH4Br (110) Surface, Physical Review Letters 71 (1993) 1188.

[33] D. Cellai, A. Lawlor, K. A. Dawson, J. P. Gleeson, Tricritical point in heterogeneous k-core percolation (2011).

[34] S. Alexander, R. Orbach, Density of states on fractals : "fractons", Journal de Physique Lettres 43 (1982) 625.

[35] S. Kirkpatrick, Percolation and Conduction, Reviews of Modern Physics 45 (1973) 574.

6

Application of the developed model to VGCNF/Epoxy and CNT/Thermoplastic composites

This chapter is based on the discussion of the theoretical results presented in [1] and in [2]. The developed model presented in the previous chapters is applied to systems obtained with different dispersion methods for CNT [1] in a Epoxy resin. The model is also applied to CNT dispersed in a thermoplastic, poly(vinylidene fluoride) (PVDF), with different surface treatments. The experimental details can be found in [1] and [2], respectively.

6.1 VGCNF/Epoxy composites

In this section the previously developed model is applied to VGCNF/Epoxy prepared with four dispersion methods. It is shown that each method induces a strong influence on the composite electrical properties that can be captured by the developed model. It is also found that the conductivity can be described by a weak disorder regime, for the different dispersion methods.

This section is based on the theoretical results presented in [1] where the experimental details are also described.

The results for the DC and AC conductivity (1kHZ) are summarized in Fig. 6.1 as a function of the VGCNF volume fraction for the different methods in, as shown in Fig. 6.1.

In the samples prepared by Methods I and II, the AC conductivity demonstrates an increase of five and six orders of magnitude for volume fractions of 6E-4 and 3E-3 respectively (Fig. 6.1, left). Moreover, the same samples also reveal a strong increase in the DC conductivity of 6 and 8 orders of magnitude respectively, at similar volume fractions (Figure 6.1, right). In fact, the highest conductivity values are achieved with these two methods. When using Method III to disperse the VGCNF, both the AC and DC conductivities are very low and almost independent of the volume fraction. This behaviour can be related to the formation of a capacitive network [3, 4] as discussed below in

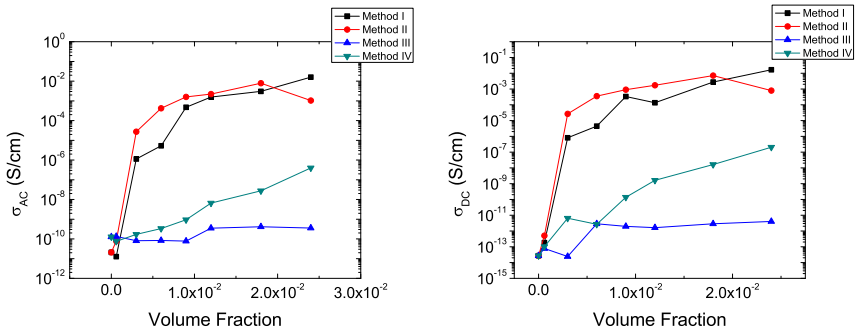

Figure 6.1: Log-linear plot of the conductivity versus volume fraction for the different dispersion methods.Left - AC conductivity (1 kHz); Right - DC conductivity.

this section. In the case of Method IV, the composites conductivity (AC and DC) shows a slight increase with volume fraction, but the highest value is only three orders of magnitude higher than the AC conductivity and seven orders of magnitude higher than the DC conductivity of the epoxy resin, respectively. Furthermore, no percolation threshold was found.

The percolation theory also predicts a power law relationship between conductivity and volume fraction as described by Equation (3.1). Fits of Equation (3.1) to the data of Fig. 6.1 were inconclusive. For fibres with a capped cylinder shape, in general, the percolation threshold is defined within the following bounds described by Equation (2.1). Using the values provided by the manufacturer of the VGCNF [1], Equation (2.1) predicts the bound $2E-3 \leq \Phi_c \leq 3E-3$ for an average aspect ratio of 433. The Φ_c found in this work for Methods I and II ($6E-4 \leq \Phi_c \leq 3E-3$) includes the predictions of the theory, with exception of the upper bound. This indicates that a network is formed, but it does not necessarily imply a physical contact between the VGCNF.

Through the application of the network theory to VGCNF composites, namely by mapping fillers to vertices and edges to the gaps between fillers, a formula relating the composite conductance to the network disorder, Equation (4.8), has been deduced in Chapter 4. Equation (4.8) can be tested, as explained in Chapter 4, by fitting $\log(\sigma) \sim \Phi^{-\frac{1}{3}}$ to the experimental values. The latter dependence was tested for the composite AC conductivity at 1 kHz (Fig. 6.2 , left), and for the DC measurements (Fig. 6.2, right).

As can be observed in Fig. 6.2, there is a linear relation between the logarithm of the conductivity and the volume fraction for Methods I and II. This indicates that the composite conductivity is in the weak disorder regime [5]. On the other hand, the data for Method IV shows the same linear behavior,

[1] Applied Sciences Inc., Available from: http://www.apsci. com/ppi-pyro3.html.

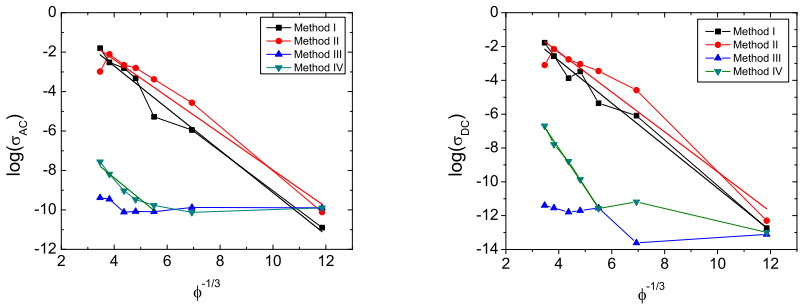

Figure 6.2: Left - Logarithm of the AC conductivity at 1 kHz versus volume fraction for the different mixing methods. The thick lines are linear fits to the data $\left(R^2 \sim [0.97, 0.95, 0.91]\right)$. Right - Logarithm of the DC conductivity versus volume fraction for the different methods. The thick lines are linear fits to the data $\left(R^2 \sim [0.98, 0.92, 0.99]\right)$.

but only for the higher volume fractions and deviating for the lower volume fractions. This deviation from the linear relation can be described by Equation (4.8), when the conductive network is not yet formed, which implies that the effective conductance is controlled by the matrix conductance [5]. This fact indicates that the network is only formed by capacitors in lower volume fractions and the matrix dominates the overall conductivity.

Hopping between nearest fillers explains the deviation from the percolation theory; the overall composite conductivity being explained by the existence of a weak disorder regime. The formation of a capacitor network [4], where the plates of each capacitor are VGCNF pairs, explains the deviation from the expected linear relation between the logarithm of the conductivity and volume fraction, as predicted by the weak disorder regime. It is also associated to the better filler dispersion, characteristic of Methods III and IV, as demonstrated by the SEM images presented in [1]. On the other hand, a good distribution of the clusters, characteristic of Methods I and II [1], results in better conducting properties.

6.2 CNT/Thermoplastic composites

This section is based on the results presented in [2] where the experimental details are described.

In the work presented in this section it is discussed the application of the developed theoretical model to CNT/PVDF composites prepared using CNT with different oxidation and thermal treatments. The surface treatments, in general, increase the percolation threshold and decrease conductivity. It is

demonstrated that the composite conductivity can be attributed to a hopping mechanism that is strongly affected by the surface treatment of the CNT.

In Fig. 6.3 shows the concentration dependence of the DC conductivity for the different composites.

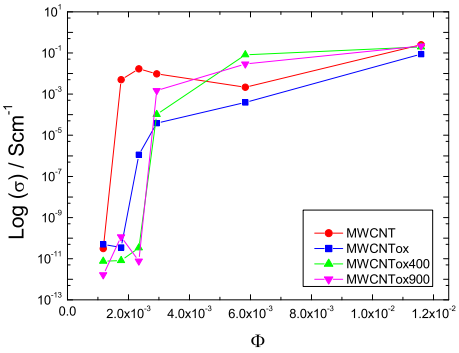

Figure 6.3: DC conductivity (σ) as function of the volume fraction (Φ) for different functionalized MWCNT.

In Figure 6.3 it is presented the results for the DC conductivity and as can be seen the pristine MWCNT have a lower percolation threshold than the functionalized ones, which is in contrast with the same percolation threshold, for the pristine and functionalized MWCNT, obtained in other studies [6, 7]. The latter authors explain the higher conductivity that is achieved by the pristine MWCNT by a reduction on the length of the MWCNT. It is important to notice that if there is a reduction in the length of the MWCNT, different percolation threshold should be also observed, which is not the case from the latter works. As the conductance of the MWCNT is mainly determined by the π orbitals [8], when the MWCNT are surfaced treated or functionalized and the functional groups or defects are related to the π orbitals, the conductance of the MWCNT is lowered and therefore the functionalized composites should demonstrate, in general, a lower conductivity.

A more quantitative assessment of the electrical properties was achieved by analysing the results of Fig. 6.3 with Equation (3.1) from the percolation theory, but the obtained results are inconclusive, indicating that the theory is not appropriate for a proper description of the observed behaviour. Then, a description based on the network theory was applied, that relates the composite conductance to the network disorder, by mapping fillers to the vertices of the network and edges to the gaps between the fillers as described in [5]. The latter network assumption results in Equation (4.8) that can be tested, as explained in Chapter 4, by fitting $\log(\sigma) \sim \Phi^{-\frac{1}{3}}$ to the experimental values. The latter

dependence was tested for the composites DC conductivity and it is presented in Fig. 6.4.

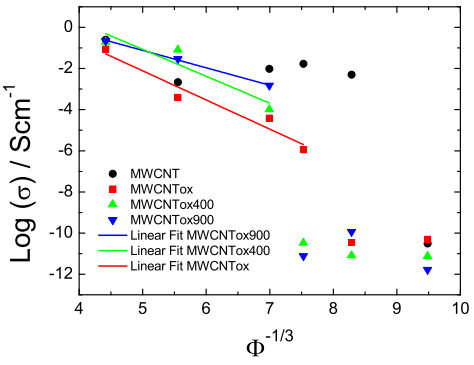

Figure 6.4: Logarithmic plot of the DC conductivity (σ) as function of the volume fraction (ϕ). Thick lines are linear fits to the presented data, $R^2 \sim 0.9$

As can be observer in Fig. 6.4, there is a linear relation between the logarithm of the conductivity, but only for the higher volume fractions. A deviation from this behaviour was observed for the lower volume fraction and for the composites prepared with pristine MWCNT. This indicates that the composite conductivity is in the weak disorder regime [5], as the $\log(\sigma) \sim \Phi^{-\frac{1}{3}}$ is observed. The deviation form the linear relation can described by Equation (4.8), when the conductive network is not yet formed, which implies that $G_{eff} = G_{cutt}$ [5], i.e. the effective conductance is controlled by the matrix conductance. This fact indicates that the network is only formed by capacitors at the lower volume fractions and the matrix dominates the overall conductivity.

As a conclusion hopping between nearest fillers explains the deviation from the percolation theory and the overall composite conductivity is explained by the existence of a weak disorder regime. The formation of a capacitor network for the lower filler concentrations [4], where the plates of each capacitor are MWCNT pairs, explains the deviation from the expected linear relation between the logarithm of the conductivity and volume fraction, as predicted by the weak disorder regime. On the other hand, the fact that the linear relation is not present in the composites prepared with pristine MWCNT indicates that the surface treatment of the CNT determines the nature of the transition of the isolator to the conductive regime, as well as the conduction mechanism of the composites.

6.3 Conclusion

It can be conclude that the developed model can be applied to different system successfully, enabling the understanding of the conduction mechanism.

6.4 References

[1] P. Cardoso, J. Silva, D. Klosterman, J. A. Covas, F. W. J. V. Hattum, R. Simoes, S. Lanceros-mendez, The role of disorder on the AC and DC electrical conductivity of vapour grown carbon nanofibre / epoxy composites, Composites Science and Technology 72 (2012) 243–247.

[2] S. A. C. Carabineiro, M. F. R. Pereira, J. Nunes-Pereira, J. Silva, C. Caparros, V. Sencadas, S. Lanceros-Méndez, The effect of nanotube surface oxidation on the electrical properties of multiwall carbon nanotube/poly(vinylidene fluoride) composites, Journal of Materials Science 47 (2012) 8103.

[3] R. Simoes, J. Silva, S. Lanceros-Mendez, R. Vaia, Influence of fiber aspect ratio and orientation on the dielectric properties of polymer-based nanocomposites, Journal of Materials Science 45 (2009) 268.

[4] R. Simoes, J. Silva, R. Vaia, V. Sencadas, P. Costa, J. Gomes, S. Lanceros-Mendez, Low percolation transitions in carbon nanotube networks dispersed in a polymer matrix: dielectric properties, simulations and experiments, Nanotechnology 20 (2009) 35703.

[5] J. Silva, R. Simoes, S. Lanceros-Mendez, R. Vaia, Applying complex network theory to the understanding of high aspect ratio carbon filled composites, Europhysics Letters (EPL) 93 (2011) 37005.

[6] Q. Li, Q. Z. Xue, X. L. Gao, Q. B. Zheng, Temperature dependence of the electrical properties of the carbon nanotube/polymer composites, eXPRESS Polymer Letters 3 (2009) 769–777.

[7] Q. Li, Q. Xue, Q. Zheng, L. Hao, X. Gao, Large dielectric constant of the chemically purified carbon nanotube/polymer composites, Materials Letters 62 (2008) 4229–4231.

[8] J.-C. Charlier, X. Blase, S. Roche, Electronic and transport properties of nanotubes, Reviews of Modern Physics 79 (2007) 677.

7

Conclusions and future developments

7.1 Conclusions

This thesis was devoted to the study of the electrical and dielectric response of polymer composites where the reinforcements are high aspect ratio carbon allotropes.

The thesis starts by exploring the dielectric constant of CNT/polymer composites. It was found that an increase of the aspect ratio of the fillers increases the dielectric constant of the nanocomposite for a given volume fraction, supporting experimental results for the dielectric constant in nanocomposites [1]. It was demonstrated that nematic materials show a lower dielectric constant when compared to isotropic ones. This behaviour that had previously been found experimentally for the electrical conductivity [2]. It was concluded that for nematic state materials with different aspect ratios, the dielectric constant follows a power law. The difference in the aspect ratios is reproduced in the power law scaling constant and the power law exponent remains unchanged, suggesting that it is related to the filler distribution and degree of anisotropy.

With respect to the study of the electrical conductivity of CNT/polymer nancomposites, a model based in "hard-core" cylinders was constructed and it was demonstrated that simulations based on hard-core cylinders can describe the conductivity of the nanocomposites. The latter simulations demonstrate that increasing aspect ratio increases the electrical conductivity. On the other hand, increasing anisotropy will decrease conductivity; this effect being more evident at higher volume fractions. Finally, it was demonstrated that the alignment of rods parallel to the measurement direction results in higher conductivity values, in agreement to recent experimental work [3].

It was shown that the microstructure generated by a derivation of sequential packing algorithm can be described by a random graph, where the vertices correspond to rods and the edges to the junction between them. This approach is not limited to rod-like fillers and can be extended to other fillers with different geometry. It is also shown that the conduction in VGCNF/polymer composites

can be described by a Bethe lattice confirming recent experimental results [4]. Through the use of the complex network framework, an expression was obtained for the percolation threshold. In the same way, it was demonstrated that hopping between adjacent fillers gives rise to an expression, $\log(\sigma_{DC}) \sim \Phi^{-\frac{1}{3}}$, that corresponds to a weak disorder regime.

The critical exponents for a hard-core 3D cylinder system with short-range interactions have been obtained making use of the network theory, and these are related through the common hyperscaling for a 3D system. In contrast to the 2D stick system and the 3D hard-core cylinder system, the determined critical exponents do not belong to the same universality class as the lattice percolation. Instead, the correlation length critical exponent has a typical mean field value, the γ critical exponent has a value that is close to the mean field one, and $\beta = 0.3$. Interestingly, using the Alexander-Orbach conjuncture, it was found that the relation between the conductivity and the correlation length critical exponents for a 3D system is obeyed.

The model developed based on network theory, where the polymer reinforcement is mapped to vertices and the interaction between them to the network edges,was applied to VGCNF/epoxy composites prepared with different dispersion methods [5] and to composites consisting on CNT with different surface treatments dispersed in thermoplastic poly(vinylidene fluoride) [6]. It was found that for VGCNF/Epoxy composites the dispersion methods induce a strong influence on the composite electrical properties that can be captured by the model. It was also found that the electrical conductivity can be described by a weak disorder regime, a regime where all fiber-fiber conductive links participate in the overall composite conductance.

For CNT/PVDF composites prepared using CNT with different oxidation and thermal treatments it was found that he surface treatments increase the percolation threshold and decrease conductivity. It was also demonstrated that the composite conductivity can be attributed to a hopping mechanism that is strongly affected by the surface treatment of the CNT.

It can thus be concluded that the inclusion of conductive fillers with high aspect ratio improves the dielectric and electric response of a polymer and that this response can be modeled using a network approach. The developed model provides insights on the composite response with varying orientation and volume fraction of added fillers. This network of fillers has non trivial critical exponents with the conductive critical exponent being similar to the mean field one.

With this work, a deeper understanding of the electric and dielectric response of polymer composites high aspect ratio conductive fillers, mainly CNT and VGCNF, has been achieved. The developed model can now be used as a

predictive tool to fabricate composites with tailored properties, such as the ones needed for piezoresistive and/or capacitive sensors, in which the filler content, type and orientation play a critical role in composite response and therfore in their suitability for the intended application.

7.2 Future developments

This thesis focused on the study of the electrical and dielectric properties of dispersed high aspect ratio fillers in a polymer matrix. In the future the developed methodology can be applied to clusters of fillers distributed in a polymer matrix to study how the cluster formation influences the composite electric and dielectric response. Further, it is necessary the study of how the size, number and distribution of clusters influences the overall composite response.

7.3 References

[1] S.-H. Yao, Z.-M. Dang, M.-J. Jiang, H.-P. Xu, J. Bai, Influence of aspect ratio of carbon nanotube on percolation threshold in ferroelectric polymer nanocomposite, Applied Physics Letters 91 (2007) 212901.

[2] F. Du, J. Fischer, K. Winey, Effect of nanotube alignment on percolation conductivity in carbon nanotube/polymer composites, Physical Review B 72 (2005) 121404.

[3] A. Dombovari, N. Halonen, A. Sapi, M. Szabo, G. Toth, J. Mäklin, K. Kordas, J. Juuti, H. Jantunen, A. Kukovecz, Moderate anisotropy in the electrical conductivity of bulk MWCNT/epoxy composites, Carbon 48 (2010) 1918–1925.

[4] A. Trionfi, D. H. Wang, J. D. Jacobs, L. S. Tan, R. A. Vaia, J. W. P. Hsu, Direct Measurement of the Percolation Probability in Carbon Nanofiber-Polyimide Nanocomposites, Physical Review Letters 102 (2009) 116601.

[5] P. Cardoso, J. Silva, D. Klosterman, J. A. Covas, F. W. J. V. Hattum, R. Simoes, S. Lanceros-mendez, The role of disorder on the AC and DC electrical conductivity of vapour grown carbon nanofibre / epoxy composites, Composites Science and Technology 72 (2012) 243–247.

[6] S. A. C. Carabineiro, M. F. R. Pereira, J. Nunes-Pereira, J. Silva, C. Caparros, V. Sencadas, S. Lanceros-Méndez, The effect of nanotube surface oxidation on the electrical properties of multiwall carbon nanotube/poly(vinylidene fluoride) composites, Journal of Materials Science 47 (2012) 8103.